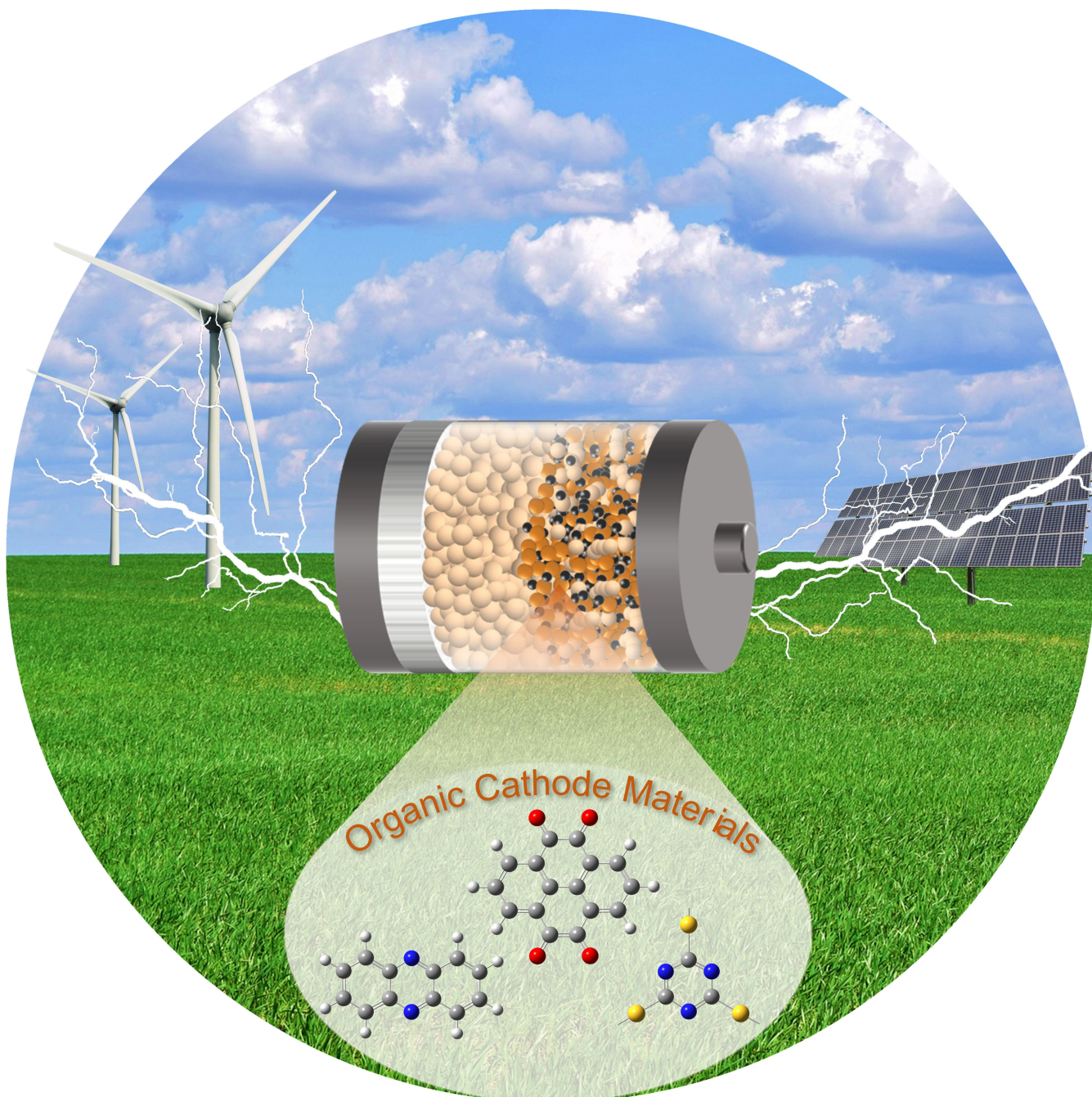


Solid-State Batteries Based on Organic Cathode Materials

Xiaotang Gan⁺^[a], Zihao Yang⁺^[a] and Zhiping Song*^[a]



Organic cathode materials (OCMs) possess high resource sustainability, large structural diversity, high theoretical energy density, and potentially low cost, however, suffer from the dissolution problem in liquid non-aqueous electrolyte. Solid-state batteries (SSBs) are regarded as the final solution of Li and Na metal batteries because of the intrinsic safety, but hindered by many challenges including the poor contact with rigid inorganic cathode materials. Therefore, applying OCMs in SSBs is probably a win-win strategy to compensate for their respective deficiency. In this review, some fundamental knowl-

edge of OCMs and SSBs are briefly introduced at first, with emphasis on different types of solid-state electrolytes (SSEs). Then the reported works on OCM-based SSBs are summarized by classifying them into non-ceramic, semi-ceramic, and all-ceramic ones. Finally, we conclude our understandings on the main scientific issues and possible solutions. To sum up, the combination of OCMs and SSBs brings about many new challenges but also opportunities towards their practical application.

1. Introduction

Rechargeable batteries have been recognized as one of the most competitive electrical energy storage technologies and their development never stops. From lead-acid batteries ($\sim 35 \text{ Wh kg}^{-1}$) invented in 1859, to nickel–cadmium batteries ($\sim 40 \text{ Wh kg}^{-1}$), nickel–metal hydride batteries ($50\text{--}80 \text{ Wh kg}^{-1}$), and today's widely used lithium-ion batteries (LIBs, $150\text{--}300 \text{ Wh kg}^{-1}$), battery technologies are mainly driven by the pursuit of higher energy density.^[1] In spite of the great commercial success of LIBs, the energy density based on intercalation chemistry is theoretically limited to 400 Wh kg^{-1} .^[2] In order to further increase the energy density, lithium (Li) metal anode has to be applied, which brings about many new challenges and opportunities.^[3] On one hand, the safety and rechargeability issues of Li metal anode have given rise to solid-state batteries (SSBs) as an alternative to conventional liquid-electrolyte batteries. On the other hand, the cost and resource sustainability issues of Li and scarce transition metals (e.g., cobalt and nickel) promote the development of rechargeable sodium (Na) batteries^[4] as well as nonmetallic sulfur (S),^[5] oxygen (O_2),^[6] and organic cathodes^[7] that have to be matched with Li or Na metal anode.

Organic cathode materials (OCMs) are composed of naturally abundant elements including C, H, O, N, and S, and possess many advantages including diverse and designable structures, high theoretical capacity (up to 600 mAh g^{-1}) and energy density (up to 1000 Wh kg^{-1}), potentially low cost, and wide applications (almost in all kinds of rechargeable batteries).^[8] During the last half-century and especially the last two decades, numerous kinds of electroactive organics have been reported as OCMs for various types of rechargeable batteries, especially Li and Na metal batteries. However, the practical applications of OCMs, especially the intensively investigated n-type ones (will be explained later), face three major challenges. First, it is almost unavoidable for small molecules and low-molecular-weight polymers (including their

discharged forms) to dissolve in liquid non-aqueous electrolytes and thereby cause poor cycling stability.^[9] Second, the poor electronic conductivity and low mass density ($1\text{--}2 \text{ g cm}^{-3}$) make it necessary to add a large amount of conductive carbon in the electrode for ensuring the full utilization of OCM, which significantly reduces the gravimetric and volumetric energy density at the electrode and cell level.^[10] Third, as the primary application orientation, Li/Na-organic batteries rely on a thorough settlement of the safety and rechargeability problems of Li and Na metal anodes.

Besides, although SSBs are regarded as the final solution of Li and Na metal batteries because of the intrinsic safety, there is still a long way to get practical application, especially for all-solid-state batteries (ASSBs) that can work at room temperature. The main obstacles include the insufficient ionic conductivity and electrochemical window of solid-state electrolytes (SSEs), as well as the poor physical contact, chemical compatibility, and electrochemical compatibility between electrolyte and cathode or anode active material.^[11] Especially, for conventional transition-metal-based inorganic cathodes, it is difficult for the SSE to form intimate contact with the rigid crystal particles and remain electrochemically stable at high charging potential (4.0–4.5 V vs. Li^+/Li). Moreover, with a look at the sustainability, it is urgent to develop other cathode materials for SSBs without relying on scarce metals.

In this context, the combination of OCMs and SSBs is probably a win-win strategy to compensate for their respective deficiency.^[12] First, the non-mobility of SSEs completely prevents the dissolution of OCMs and their shuttle between cathode and anode. Second, the intrinsic safety of SSBs will realize the practical application of Li and Na metal anodes, which is essential for the practical application of OCMs. Third, the higher flexibility and processability of OCMs than rigid inorganics are more preferred for intimate contact with SSEs. Fourth, compared with inorganic cathodes, the moderate redox potentials of OCMs request significantly lower oxidation potentials of the SSEs (3.0–4.0 V vs. Li^+/Li). Fifth, compared with other abundant cathode materials like S and O_2 , OCMs possess faster redox kinetics and smaller volume variation during discharge-charge process.

Benefiting from all the above advantages, SSBs based on OCMs attract increasing research attentions in recent five years.^[13] Although the study is still in its infant stage, it is necessary to summarize the fundamental knowledges and

[a] X. Gan,⁺ Dr. Z. Yang,⁺ Prof. Z. Song
Hubei Key Lab of Electrochemical Power Sources
College of Chemistry and Molecular Sciences
Wuhan University
Wuhan 430072 (China)
E-mail: zpsong@whu.edu.cn

[+] These authors contributed equally to this work.

research progress in this field at present. In this review, we firstly introduce some basic knowledges of OCMs and SSBs separately, including the working mechanisms, material classifications, and solutions for the problems. Then we summarize the reported SSB systems based on OCMs, which are classified into non-ceramic, semi-ceramic, and all-ceramic ones. Finally, we conclude our understandings and suggestions for the development of this field. Note that most of the reported examples are belong to solid-state lithium batteries (SSLBs) and only a few are solid-state sodium batteries (SSSBs), which are discussed together because of their similarities on scientific problems and solutions.

2. Organic Cathode Materials (OCMs)

2.1. Working principles of OCMs

The electrochemical redox reactions of OCMs occur through the charge state variations of the electroactive groups or moieties, while those of transition-metal-based inorganic cathode materials rely on the valence changes of the transition metals.^[14] Generally, they can be classified into n-type and p-type ones according to the electron accepting or donating property of the neutral molecule.^[15] As shown in Figure 1(a and b), n-type OCMs tend to accept electrons and become negatively charged, while the cations (for simplicity, only alkali metal cations, $M^+ = Li^+, Na^+, K^+$, are presented in the figure, but multivalent metal cations like Mg^{2+} and Zn^{2+} , and even nonmetallic cations like H^+ and NH_4^+ are also applicable) from the electrolyte insert to compensate the charge, corresponding to the discharge or reduction process; on the contrary, p-type OCMs tend to denote electrons and become positively charged, while the anions [$A^- = ClO_4^-, PF_6^-, TFSI^-$, etc.; TFSI = bis(trifluoromethanesulfonyl)imide] from the electrolyte insert to compensate the charge, corresponding to the charge or oxidation process. In the reverse charge or discharge process, the charged molecules return back to neutral state and the

inserted cations or anions are extracted to the electrolyte. Generally, the redox potentials distribute mainly within 2.0–3.0 V vs. Li^+/Li for n-type ones and 3.0–4.0 V vs. Li^+/Li for p-type ones, depending on the chemical structures.^[16] Thus, the major application of n-type OCMs is matching with metal anodes (especially, Li and Na) to construct rechargeable metal-organic batteries, while that of p-type ones is matching with metal, graphite, or low-potential n-type organic anodes to construct dual-ion batteries.

2.2. Classifications of OCMs

During the last half-century, numerous organic compounds have joined in the OCM family. They can be categorized into small molecules, organic salts, polymers according to the structural features, or more commonly, the following types according to their electroactive groups or moieties and redox mechanisms (Figure 1c and d).

- 1) Carbonyl compounds. Benzoquinone/hydroquinone (BQ/HQ) has been long known as a famous redox couple in aqueous solutions. In fact, many other organics containing conjugated carbonyl groups can also occur reversible redox reactions, in either aqueous or non-aqueous solutions, with either H^+ or M^+ as the counterion. They mainly include quinones [e.g., anthraquinone (AQ)], diketones, dianhydrides and diimides, as well as dicarboxylates that are used as anode materials due to the relatively lower redox potentials. The universal reaction mechanism is the reversible transformation between carbonyl ($C=O$) and enolate anion ($C-O^-$), the negative charge on which is delocalized by the conjugated system. Due to the abundant chemical structures, easy material availability, diverse derivatization methods (salinization and polymerization), and high energy density (the product of reversible specific capacity and average discharge voltage), carbonyl compounds are regarded as the most favorable type of OCMs in the past two decades.



Xiaotang Gan received his B.S. degree in 2020 from College of Chemistry and Chemical Engineering, Hunan University. He is currently a Ph.D. student at College of Chemistry and Molecular Sciences, Wuhan University, under the supervision of Prof. Zhiping Song. His research focuses on high-performance organic cathode materials for rechargeable batteries.



Dr. Zihao Yang received his B.S. degree from Wuhan University of Technology in 2017, and his Ph.D. degree from Wuhan University in 2022, under the supervision of Prof. Zhiping Song. He is currently a R&D engineer at Dongfeng Motor Corporation Technical Center. His research focuses on the application of organic cathode materials in solid-state batteries.



Prof. Zhiping Song received his B.S. and Ph.D. degrees from Wuhan University, in 2006 and 2011, respectively. In 2012–2015, he worked as a postdoctoral fellow in Prof. Haoshen Zhou's group at the National Institute of Advanced Industrial Science and Technology (AIST), Japan. He is currently a professor at College of Chemistry and Molecular Sciences, Wuhan University. His research mainly focuses on organic electrode materials and their applications in various energy storage devices including lithium/sodium batteries and solid-state batteries.

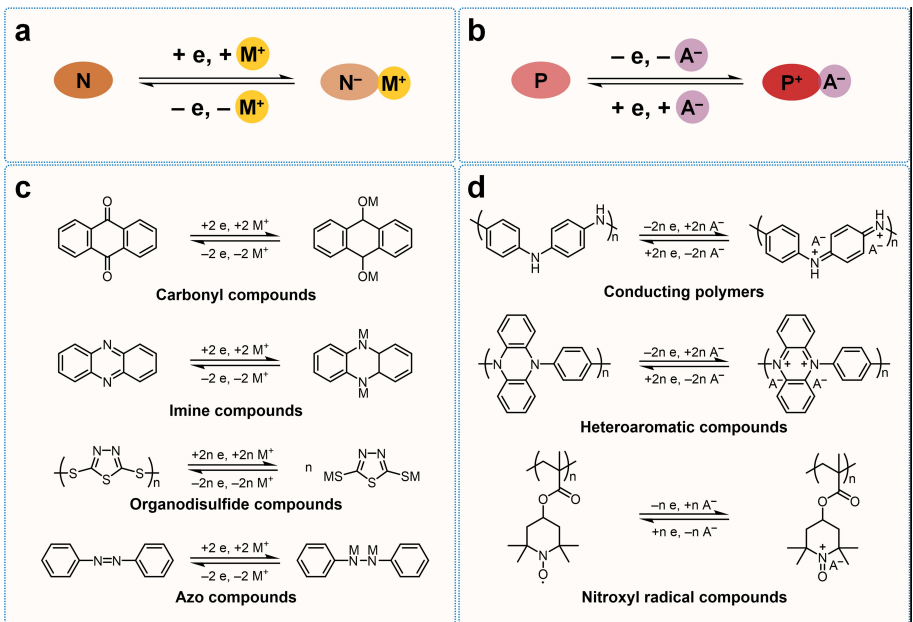


Figure 1. a, b) Schematic diagrams of the working principles and c, d) typical examples of the structures and redox reactions of the two types of OCMs: a, c) n-type; b, d) p-type. M⁺ and A⁻ mean the alkali metal cation and anion in the electrolyte, respectively.

- 2) Imine compounds. Organic molecules containing imine groups (C=N) in and out of the aromatic unit (e.g., phenazine and Schiff bases, respectively) have a similar redox mechanism to carbonyl-based materials, i.e., the reversible transformation between C=N and C=N⁻. Generally, the redox potentials of imine compounds are slightly lower than those of carbonyl ones. Although successful examples of imine-based OCMs are still limited at present, the high theoretical capacity and easy synthesis will attract more efforts to develop novel materials with high electrochemical performance.
- 3) Organodisulfide compounds. The redox mechanism of organodisulfides is the reversible breaking/rebuilding of S–S bond, which is similar to that of elemental sulfur cathode. Since 1988, a lot of organic dimers and polymers with S–S bonds have been reported,^[17] among which poly(2,5-dimercapto-1,3,4-thiadiazole) (PDMcT) is the most attractive one because of its high theoretical energy density and low cost. However, like in Li–S batteries, the discharge products of most organodisulfides (including small molecules and polymers with S–S bonds in the main chain) are easily dissolved in the electrolyte, which is even more severe than carbonyl- and imine-based OCMs.
- 4) Azo compounds. The N=N bonds in azo compounds can be electrochemically broken and rebuilt, by accepting and releasing two electrons. In 2018, a series of azobenzene derivatives were firstly reported as cathode materials for lithium batteries,^[18] among which azobenzene-4,4'-dicarboxylic acid lithium salt (ADALS) showed the best electrochemical performance.^[18c] Although one N=N bond delivers double of electrons of one C=O or C=N bond, its relatively lower redox potential (e.g., ~1.5 V vs. Li⁺/Li for ADALS) limits the application of azo compounds as OCMs.
- 5) Conducting polymers. When conducting polymers were discovered in 1970s and 1980s for their exceptional electronic conductivity, they were also found electrochemically active and applicable as cathodes for rechargeable batteries.^[15] The representatives include polyaniline (PAni), polythiophene (PTh), and polypyrrole (PPy), which mainly possess p-type behaviors at above 3.0 V vs. Li⁺/Li. The positive charge is mainly concentrated on heteroatoms like N and S, and can be delocalized along the polymer chain. Due to the unstable chemical structures of them and the oxidation decomposition of electrolytes at high potential (e.g., >4.2 V vs. Li⁺/Li), the practical capacities of conducting polymers are generally limited to 100–200 mAh g⁻¹, even when neglecting the considerable mass of doped anions from the electrolyte.^[19]
- 6) Heteroaromatic compounds. Many heteroaromatic compounds with O, N, and S heteroatoms have a similar redox mechanism to conducting polymers, but possess not high electronic conductivity like them. The representative structure units include N-substituted phenazine, phenothiazine, phenoxazine, thianthrene, and viologen. Some of these structures, e.g., N-substituted phenazine and viologen, have relatively lower redox potentials, and thus able to fully utilize the two-electron reaction to achieve higher capacities than conducting polymers.
- 7) Nitroxyl radical compounds. As one of the famous stable radicals, 2,2,6,6-tetramethylpiperidine-1-oxyl (TEMPO) possesses the reversible transformation between >N–O[•] radical and >N⁺=O cation, therefore it can be used as a p-type structure unit of OCMs. Since 2002, a lot of TEMPO-containing polymers have been reported as cathodes for rechargeable Li batteries, among which poly(2,2,6,6-tetramethylpiperidine-1-oxyl-4-yl methacrylate) (PTMA) is

the most intensively investigated one.^[20] Benefiting from the rapid electron self-exchange between adjacent TEMPO radicals, these polymers have very fast reaction kinetics and thus high rate capability,^[21] but the theoretical capacities are less competitive than other p-type OCMs (e.g., 112 mAh g⁻¹ for PTMA).

Due to the structure diversity and designability of OCMs, the above categories cannot take in all reported structures. For instance, there are a few scattered examples of nitrile compounds,^[33] nitro compounds,^[34] and sulfonamide salts^[35] reported as n-type OCMs in recent years. Moreover, some electroactive groups and moieties can be combined together for higher energy density. For example, C=N groups have been widely used to connect C=O-containing units for larger conjugated structure and higher theoretical capacity.^[36] We hope that this simple introduction can help beginners in this field to have a preliminary understanding of OCMs so as to read the subsequent contents smoothly. Readers who want to know more about OCMs are recommended referring other reviews focusing on this topic.^[8,9,10,14]

2.3. Strategies against dissolution problem of OCMs

Even though numerous OCMs have been reported in the past half-century, only a few among them demonstrate satisfactory cycling performance under common test conditions without special treatment or optimization on the electrode, electrolyte, and separator. The main problem is that for small molecules

and even polymers with relatively lower molecular weight (i.e., oligomers), it is almost unavoidable for the active material (at the pristine state or different depth of discharge/charge) to dissolve in commonly used non-aqueous electrolytes during discharge-charge process. It leads to not only the loss of active material from the cathode, but also the migration of dissolved species to the anode side, and the subsequent side reactions on the anode surface and shuttling between anode and cathode (in charging process, the dissolved species at higher oxidation state diffuse to the anode and are electrochemically reduced, and then the species at lower oxidation state transport back to the cathode and are oxidized again). These behaviors cause incomplete realization of the theoretical capacity, fast capacity fading, low Coulombic efficiency, and even poor stability of the anode. Recently, the Song group found that many small-molecule organic cathode materials (SMOCMs) have significantly different solubilities at different discharge/charge states, and thus it is quite common to observe a dissolution-redeposition phenomenon during discharge-charge process.^[25a,37] It causes the electrode structure evolution during cycling, which is probably more responsible for the capacity fading than the loss of active material. To solve the dissolution problem and improve the cycling stability of OCMs, numerous efforts have been devoted. In Figure 2, we summarize the main strategies and typical examples, which can be roughly categorized into two orientations, i.e., preventing the dissolution and shuttle effect in conventional liquid electrolytes, and by optimizing or changing the electrolytes. Sometimes they can be also combined together for enhanced effect.

Conventional liquid electrolytes	Concentrated electrolytes	Gel electrolytes	Solid polymer electrolytes	Solid composite electrolytes	Solid inorganic electrolytes
 X = OM, COOM, SO ₃ M (M = Li, Na, K)					
Salinization	Polymerization	3 M LiTFSI-DOL/DME	PMA/PEG-LiClO ₄ -DMSO	LiTFSI-PEO	LiTFSI-PEO/PEG-γ-LiAlO ₂
		4 M NaOTf-G3	PVDF-HFP-LiTFSI-NMP	NaFSI-PPC-cellulose-nonwoven	LiTFSI-PEO-LLZTO
					Li ₇ P ₃ S ₁₁

Figure 2. Typical strategies and examples of inhibiting dissolution of OCMs in different types of electrolytes. The optimal strategies against the dissolution of OCMs in conventional liquid electrolytes include salinization,^[22] polymerization,^[16] immobilization^[23] and blocking.^[24] The full names of the compounds are listed below: PTCDA, 3,4,9,10-perylenetetracarboxylic dianhydride;^[25] AQ, 9,10-anthraquinone;^[26] C4Q, calix[4]quinone;^[27] THQAP, 2,3,9,10-tetrahydroxyquinoxalino[2,3-b]phenazine-6,13-dione;^[28] TMQ, tetramethoxy-p-benzoquinone;^[29] TCAQ, 11,11,12,12-tetracyano-9,10-anthraquinonedimethane;^[30] Li₂Q, lithiated p-benzoquinone;^[31] PTTCA, poly(trithiocyanuric acid).^[32] The full names of electrolyte salts are listed below: LiTFSI, lithium bis(trifluoromethanesulphonyl)imide; NaOTf, sodium trifluoromethanesulfonate; NaFSI, sodium bis(fluorosulfonyl)imide; LLZTO, Li_{6.4}La₃Zr_{1.4}Ta_{0.6}O₁₂. The full names of electrolyte solvents or polymers are also listed below: DOL, 1,3-dioxolane; DME, 1,2-dimethoxyethane; G3, triethylene glycol dimethyl ether; PMA, phenylmercuric acetate; PEG, polyethylene glycol; DMSO, dimethyl sulfoxide; PVDF-HFP, poly(vinylidene fluoride-co-hexafluoropropylene); NMP, N-methylpyrrolidone; PEO, polyethylene oxide; PPC, poly(propylene carbonate).

For the application of OCMs with conventional liquid electrolytes, the main methods include salinization, polymerization, immobilization, and blocking. Salinization, i.e., functionalizing SMOCMs with phenate ($-OM$),^[22a-d] carboxylate ($-COOM$),^[22e-j] and sulfonate ($-SO_3M$) ($M=Li, Na, K$)^[22k,l] groups, etc., can usually enhance the crystal structure stability through the introduced $O\cdots M\cdots O$ ionic/coordination bonds. Besides, polymerization is used to connect the electroactive units through covalent bonds, which is fundamentally more effective to prevent the dissolution, i.e., the polymer is absolutely insoluble if the molecular weight is high enough. For example, BQ can be polymerized by connecting the monomers through $-CH_2-$, $-NH-$, $-O-$, and $-S-$ linkers,^[16] which will not reduce the theoretical capacity too much. Although the two methods can enhance the insolubility of the OCM itself and alleviate or even completely solve the dissolution problem, it is a huge challenge to rationally design and precisely synthesize the material, especially when considering the cost of synthesis and loss of theoretical capacity.

Besides the structure of active material, strategies can also focus on the structures of electrode and separator. In this respect, immobilization and blocking are two main methods, the effect of which have been widely proved in Li-S batteries. For example, compositing SMOCMs with mesoporous carbon is useful to alleviate the dissolution through physical confinement.^[23] Moreover, using ion permselective membrane (e.g., SSEs and Nafion) as separator is an effective approach to block the transport of dissolved species (with excessive size and/or opposite charge) from the cathode to the anode.^[24] Although it is useless to inhibit the dissolution, the shuttle effect can be significantly eliminated, which is also very helpful to improve the cycling performance and especially the Coulombic efficiency. Compared with the molecular engineering strategies, the two methods are more universal for different SMOCMs. However, they will also largely increase the cost and reduce the energy density at the electrode and cell levels.

Since dissolution is the interaction between OCM and electrolyte, the electrolyte plays a crucial role in influencing the solubility and dissolution-redeposition behaviors. Therefore, in addition to using conventional liquid electrolytes, researchers have also attempted to modify or change the electrolytes for OCMs. In Figure 2, the novel electrolytes are classified into concentrated, gel, solid polymer, solid composite, and solid inorganic ones, roughly in the order of increasing solid and inorganic features. Encouraged by the efficacy of using highly concentrated electrolytes in Li-S batteries,^[40] research have also attempted to increase the concentration of commonly used ether-based electrolytes for SMOCMs, which can reduce the content of free solvent molecules and increase the viscosity to suppress the dissolution. For example, Cai et al.^[25a] found that 3,4,9,10-perylenetetracarboxylic dianhydride (PTCDA; Figure 2) exhibited excellent cycling performance in the 3 M LiTFSI-DOL/DME electrolyte. At a higher concentration of 4 M, the cycling stability of PTCDA became even poor, indicating that absolute insolubility is probably adverse to the electrochemical performance of SMOCMs. It is speculated that the diffusion of Li^+ ions in the organic crystalline bulks is rather slow, which can be

significantly accelerated after partial dissolution. It is an important issue for the application of SMOCMs in SSBs and should be investigated in depth in the future. The gel electrolyte is formed by confining liquid electrolyte in a polymer framework, and the ion conduction dominantly occurs in the liquid phase. Although some researchers also called it quasi-solid-state electrolyte, it is necessary to distinguish it from those using SSEs for ion conduction and liquid additive for wetting the interfaces. Since the polymer framework can reduce the mobility of liquid electrolyte as well as dissolved organic species from the cathode, it is reasonable to expect gel electrolytes to alleviate the dissolution problem and shuttle effect of SMOCMs. A successful example is that, Huang et al.^[27] applied the PMA/PEG-LiClO₄-DMSO gel electrolyte to test calix[4]quinone (C4Q; Figure 2) and obtained greatly improved electrochemical performance compared to that with conventional liquid electrolyte. Furthermore, SSEs are more efficient to fully solve the dissolution problem of OCMs, which will be emphatically discussed in the subsequent sections.

3. Solid-State Batteries (SSBs)

Solid-state batteries (SSBs) are attracting extensive attentions because of the pursuit of energy storage devices with both high energy density and safety, which contradict each other to some extent. As an alternative of volatile and inflammable liquid organic electrolytes, SSEs possess preferable thermal stability and mechanical strength, and thus can avoid liquid leakage, flatulence, and explosion, even when the thermal runaway takes place.^[41] Moreover, using SSEs is probably the most effective approach to suppress the metal dendrite growth and penetration so far, and thus it provides the prospect of the practical application of Li and Na metal anodes. It can not only further increase the energy density of batteries using conventional inorganic cathodes, but is also indispensable for the practical application of S, O₂, and n-type organic cathodes. In addition, compared to liquid electrolytes, SSEs still have many other unique advantages: 1) high transference number of Li^+ or Na^+ ion (usually close to 1) for avoiding the concentration polarization in high-rate discharge-charge process; 2) high thermal stability and enhanced ionic conductivity for working at higher temperature; 3) non-mobility for eliminating the penetration and shuttle effect of dissolved electroactive species; 4) the relatively sluggish and impersistent solid-phase side reactions for extending the battery life.^[50]

3.1. Classifications of solid-state electrolytes (SSEs)

Since 1960s,^[51] numerous SSEs of Li^+ and Na^+ ions have been developed with ever-increasing ionic conductivity. Given their composites, structures, and properties, they can be broadly divided into three categories: solid inorganic electrolytes (SIEs, also called as ceramic electrolytes), solid polymer electrolytes (SPEs), and solid composite electrolytes (SCEs) (Figure 3).^[38,39] In Table 1, we summarize the key parameters and characters of

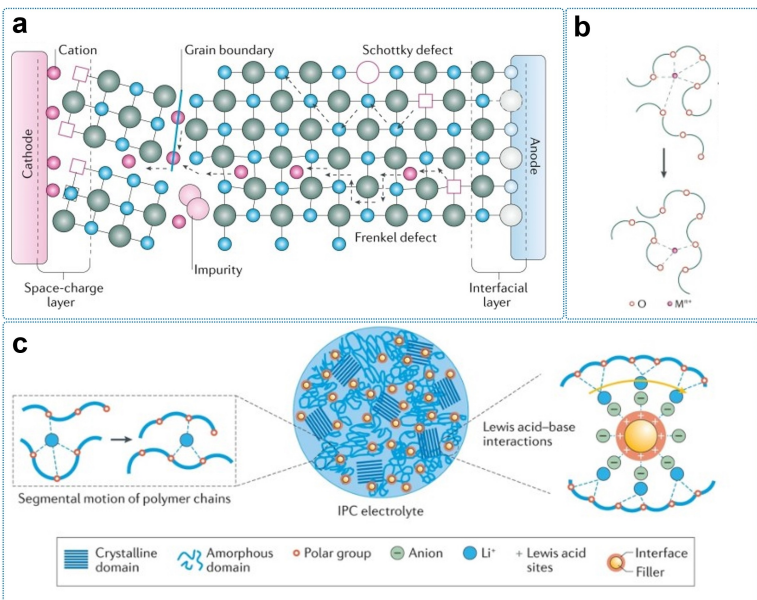


Figure 3. Ion transport mechanisms of a) SIEs, b) SPEs. Reproduced with permission from Ref. [38]. Copyright (2020) Springer Nature. c) SCEs. Reproduced with permission from Ref. [39]. Copyright (2021) Springer Nature.

the most representative and commonly used SSEs so far reported, which will be referred frequently in the following discussions. Most of them are belong to Li⁺ ion conductors, but in many cases the structures and properties are still valid when replacing Li by Na in the chemical composition, although the ionic conductivity will be probably reduced.

3.1.1. Solid inorganic electrolytes (SIEs)

In SIEs, Li⁺ or Na⁺ ions transport along with its pathways in the crystalline or amorphous bulks, with aids of the synergistic effect of its internal defects including Schottky defect and Frenkel defect (Figure 3a).^[38] The transportation is always hampered at the grain boundaries with physical voids sometimes, which should be reduced by heat pressing. Based on the ion conduction mechanism, the Li⁺ or Na⁺ ion transference number in a SIE is close to 1, which avoids the formation of concentration polarization on the anode surface and thus enables uniform Li or Na deposition. According to the chemical composition, SIEs can be roughly divided into oxides, sulfides, halides, and lithium phosphorus oxynitride (LiPON, which has been also classified into oxides in many reviews). Among them, oxide and sulfide electrolytes have been more widely used for different cathode materials including OCMs.

1) Oxide electrolytes. There are many different crystal types of oxide electrolytes, including perovskite, lithium superionic conductor (LISICON), sodium superionic conductor (NASICON), and garnet.^[52] The most representative materials include NASICON-type Li_{1.3}Al_{0.3}Ti_{1.7}(PO₄)₃ (LATP) and Li_{1.5}Al_{0.5}Ge_{1.5}(PO₄)₃ (LAGP), as well as garnet-type Li₂La₃Zr₂O₁₂ (LLZO), Li_{6.5}La₃Zr_{1.5}Nb_{0.5}O₁₂ (LLZNO) and Li_{6.5}La₃Zr_{1.5}Ta_{0.5}O₁₂ (LLZTO) (Table 1). These electrolytes usually have an ionic

conductivity of 10⁻⁴–10⁻³ S cm⁻¹ at room temperature (RT), which is not high enough for the SSBs to work at RT (the ionic conductivity is barely enough in the bulk but insufficient at the interface). The advantages of oxide electrolytes include high mechanical strength, high air and thermal stability, and relatively wide electrochemical window. However, the extreme rigidity of oxide electrolyte particles makes high-temperature sintering required to reduce grain boundary resistance and it difficult to form intimate physical contact between electrolyte and electrode layers, and between electrolyte and active material particles in the cathode composite.^[11]

- 2) Sulfide electrolytes. Typical sulfide electrolytes include glass-ceramic Li₃PS₄, Na₃PS₄, and Li₇P₃S₁₁, ceramic Li₁₀GeP₂S₁₂ (LGPS), and argyrodite-type Li₆PS₅Cl (LPSCl). Sulfur has less electronegativity and larger radius than oxygen, and thereby provides weaker binding with alkali metal ion and wider ion migration channel, respectively. Hence, sulfide electrolytes possess higher RT ion conductivity (10⁻³–10⁻² S cm⁻¹, which is approaching or even exceeding the level of liquid non-aqueous electrolytes) than oxide electrolytes and are more appropriate for SSBs working at RT. In addition, sulfide electrolytes have significantly lower rigidity or higher flexibility than oxide electrolytes, and thereby can be made into dense pellet with low grain boundary resistance and form good physical contact with active material partials just by cold pressing.^[53] However, there are two obvious drawbacks hindering their applications: narrow electrochemical window (typically 1.5–3.5 V vs. Li⁺/Li in practice^[44]) and easy deliquescence in air atmosphere.
- 3) Halide electrolytes. Halide electrolytes have a general chemical formula of Li_aMX_b, where M can be IIIA group metals (e.g., Al, Ga, In), IIIB group metals (e.g., Sc, Y),

Table 1. The key parameters and characters of representative SSEs.

Type	Material	Electrochemical window ^[a] [V vs. Li ⁺ /Li]	RT ionic conductivity ^[b] [S cm ⁻¹]	Advantages	Disadvantages
Oxide	Li _{1.3} Al _{0.3} Ti _{1.7} (PO ₄) ₃ (LATP)	2.0–4.5 ^[42]	6 × 10 ⁻⁴ ^[43]	· Wide electrochemical window · High chemical stability · High mechanical strength	· Poor flexibility · High grain-boundary resistance · High production cost
	Li _{1.5} Al _{0.5} Ge _{1.5} (PO ₄) ₃ (LAGP)	2.0–4.5 ^[42]	10 ⁻⁴ ^[43]		
	Li ₇ La ₃ Zr ₂ O ₁₂ (LLZO)	0–4 ^[11]	3 × 10 ⁻⁴ ^[11]		
	Li _{6.5} La ₃ Zr _{1.5} Nb _{0.5} O ₁₂ (LLZNO)	0–4 ^[11]	7 × 10 ⁻⁴ ^[43]		
	Li _{6.5} La ₃ Zr _{1.5} Ta _{0.5} O ₁₂ (LLZTO)	0–4 ^[11]	10 ⁻³ ^[43]		
Sulfide	Li ₁₀ GeP ₂ S ₁₂ (LGPS)	1.5–3.5 ^[44]	1.2 × 10 ⁻² ^[43]	· High ionic conductivity · Low grain-boundary resistance · Respectable flexibility	· Narrow electrochemical window · Poor compatibility with Li/Na anode · High moisture sensitivity
	Li ₂ P ₅ S ₁₁ (LPS)	1.5–3.5 ^[32,44a]	1.6 × 10 ⁻³ ^[43]		
	Li ₆ PS ₅ Cl (LPSCl)	1.5–3.5 ^[44a,45]	2 × 10 ⁻³ ^[43]		
	Na ₃ PS ₄	0.5–3.0 ^[46] (V vs. Na ⁺ /Na)	10 ⁻⁴ ^[46b]		
Halide	Li ₃ InCl ₆	1.9–4.2 ^[43]	1.5 × 10 ⁻³ ^[43]	· High ionic conductivity · High oxidation tolerance · Low grain-boundary resistance · Respectable flexibility	· High moisture sensitivity
	Li ₃ YCl ₆	0.6–4.2 ^[47]	1.7 × 10 ⁻³ ^[47]		
LiPON	Li _{3.3} PO _{3.8} N _{0.22}	0–5 ^[48]	10 ⁻⁶ ^[48]	· Wide electrochemical window	· Low ionic conductivity · Limited applicability (only for thin-film batteries) · High production cost
Polymer	LiTFSI-PEO (O:Li = 20:1)	0–4.0 ^[49]	10 ⁻⁶ ^[49]	· Wide electrochemical window · Low grain-boundary resistance · Excellent flexibility · Easy production	· Poor ionic conductivity · Poor mechanical strength · Low cation transference number

^[a] The electrochemical window values are roughly estimated after comprehensive consideration of different reports and aiming at guiding the practical use of SSEs, since they are always overestimated by voltammetry tests but underestimated by theoretical calculations. ^[b] The ionic conductivity values are mainly adopted from commercial product information, and partially estimated from different reports, aiming at guiding the practical use of SSEs.

divalent metals (e.g., Ti, V, Cr), and even non-metallic elements like N, O, and S, while X means halogen (X=Cl, Br, I).^[47] For example, Li₃YCl₆ and Li₃InCl₆ are two of the representative materials. The univalent halogen anion (X⁻) in halide electrolytes has weaker interaction with Li⁺ ions than the divalent O²⁻ and S²⁻ anions, and its larger radius leads to longer ionic bonds and larger polarizability, both of which are beneficial to ion migration in the lattice. Therefore, halide electrolytes can achieve an ionic conductivity of 10⁻³ S cm⁻¹ at RT.^[54] Moreover, because that the oxidation potentials of X⁻ are higher than that of S²⁻, halide electrolytes have a higher oxidation tolerance than sulfide electrolytes. For the similar reason, Cl⁻ is more preferred than Br⁻ to construct the halide electrolyte with wider electrochemical window. For example, Li₃YCl₆ has a 1.0 V higher oxidation potential (4.2 V vs. Li⁺/Li) than Li₃YBr₆ (3.2 V vs. Li⁺/Li).^[47] Similarly to sulfide electrolytes, halide electrolytes are also sensitive to moisture, which is an important obstacle for their synthesis and application.

4) LiPON electrolytes. LiPON is a kind of amorphous SSEs with a chemical composition of Li_aPO_bN_c, where $a=2b+3c-5$.^[55]

It has long been known for the successful application in all-solid-state thin-film batteries fabricated by atomic/molecular layer deposition (ALD/MLD). Although its ionic conductivity (10⁻⁶ S cm⁻¹ at RT) is obviously insufficient for common SSBs, the electrolyte layer in the thin-film batteries is thin enough (10–40 nm) for ensuring the ionic conduction. Besides, the electrochemical window of LiPON is also satisfactory to have a good compatibility with either Li anode or high-voltage cathode. The biggest shortcoming is that the energies of such kind of thin-film batteries are too low to be applied in our daily life.

3.1.2. Solid polymer electrolytes (SPEs)

SPEs can be regarded as the “solutions” of alkali metal salts dissolved in polymer “solvents”. The most famous example is the LiTFSI-PEO system (the O/Li molar ratio is typically 20), where PEO (polyethylene oxide) has a linear structure of H—(O—CH₂—CH₂)_n—OH and a typical average molecular weight (M_v) of 20000–50000 Da.^[11] The dissociated alkali metal cations

form coordination bonds with oxygen atoms along the polymer backbones, and transfer with the segmental motion of the polymer chains and the continuous breaking/rebuilding of the coordination bonds (Figure 3b).^[38] Since the dissociated anions (e.g., TFSI⁻) have less interaction with the polymer chains and also transfer with the segmental motion, the cation transference number is usually less than 0.5, which is a disadvantage of SPEs compared to SIEs. It is recognized that the ionic conductivity is proportional to the occupation ratio of amorphous regions in the structure, which are more dominant than crystalline regions for ion transport. Due to the unavoidable existence of crystalline regions and the relatively slow segmental motion at RT, the ionic conductivity (10^{-6} Scm^{-1}) of the LiTFSI-PEO electrolyte is obviously insufficient to enable a SSB operated at RT. Usually, the working temperature should be increased to above 60°C to obtain an acceptable electrochemical performance, or can be lowered down to about 40°C by adding plasticizers such as PEG (polyethylene glycol, or the oligomer of PEO), ionic liquid, and succinonitrile (SCN, a kind of plastic crystal). However, under such conditions, it is ambiguous whether the electrolyte is actually a solid, gel, or even liquid electrolyte. Compared to SIEs, SPEs with much higher flexibility are more favorable to form intimate physical contact with anode and cathode layers, but the much poorer mechanical strength is an obvious weakness for the battery safety, especially when reducing the thickness of electrolyte for higher energy density. For the electrochemical window, PEO is very compatible with Li and Na anode, but the electrochemical stability at high potential (>4.0 V vs. Li⁺/Li) should be improved for compatibility with high-voltage inorganic cathodes.^[48] Besides PEO and its analogues and copolymers, many other polymers like poly(propylene carbonate) (PPC) and polyacrylonitrile (PAN) have been also employed to construct SPEs,^[56] but their comprehensive performance is still less competitive than PEO.

3.1.3. Solid composite electrolytes (SCEs)

In order to improve the ionic conductivity and mechanical strength of the LiTFSI-PEO electrolyte, there were many early attempts to add various inert oxides (e.g., Al₂O₃, SiO₂, TiO₂, and ZrO₂) as nanofillers in the system, the homodisperse of which can effectively inhibit the formation of crystalline regions.^[39] However, there is a contradiction that increasing the content of these nanofillers will also block the transportation of ions. With the development of SIEs, researchers started to use them as alternative of inert oxides to construct SCEs. In addition to the enhanced ionic conduction brought by the ceramic electrolyte, the Lewis acid-base interactions between it and the functional groups on the polymer chains can also lower the ion diffusion energy barrier at the interface (Figure 3c).^[57] Therefore, the combination of SPE and SIE is a good strategy to complement each other's advantages, and thus achieve balanced ionic conductivity, electrochemical window, mechanical strength, and flexibility. According to the weight proportions of SPE and SIE in the composite, the SCEs can be roughly divided into

"ceramic in polymer" and "polymer in ceramic" types, which can be regard modifications of SPEs and SIEs, respectively. The properties of a SCE are influenced by many factors including not only the inherent structures and features of the polymer and ceramic electrolytes, but also the weight ratio, particle size, dispersity, and even fabrication methods.

3.2. Interface problems and solutions of SSBs

Although many SSEs satisfy the minimum requirement on ionic conductivity (10^{-4} – 10^{-3} Scm^{-1}), it is still difficult for them to achieve desired electrochemical performance, especially at RT or high current rate. The key reason is the problems of the interfaces, including the macroscopical ones between SSE and anode or cathode layers, and the microcosmic ones between the SSE and active material or conductive carbon particles inside the cathode layer. Briefly, the main problems at these interfaces can be divided into the following two major categories.

Physical contact. Due to the solid–solid contact and chemical–mechanical effect, the physical contact of SSE with other components is significantly poorer and less stable during discharge–charge process than that of liquid electrolyte. There are various strategies to solve this problem: 1) increasing the contact area by reducing the particle sizes of the SSE and active material and homogenizing their mixing (e.g., through ball milling); 2) adopting co-pressing and co-sintering methods to enhance the contact in the electrode and cell fabrication processes, especially for rigid SIEs and inorganic active materials;^[58] 3) maintaining external pressure during discharge–charge process to counteract the volume change of active material and electrode; 4) introducing soft buffer layer (e.g., gel electrolytes and SPEs) between the electrolyte and electrode layers;^[59] 5) introducing liquid electrolytes or additives to wet the interfaces, which can be also in-situ solidified by chemical or electrochemical methods.^[60]

Chemical and electrochemical compatibility and stability. When SSE contacts with cathode and anode active materials, they may probably react at the interfaces due to the gap between their redox states. Taking sulfide electrolytes as an example, the P⁵⁺ is easily reduced by Li and Na anode, while the S²⁻ is easily oxidized by high-voltage cathode materials. Usually, the chemical reaction leads to the formation of a thin interface layer with much higher resistance for Li⁺ or Na⁺ ion to cross (than that for diffusion in the SSE bulks), which also prevents the persistent reaction if the product is an electronic insulator (if it is an electronic conductor like metal or alloy, the interface layer will keep growing). In discharge–charge process, the participation of electrons from or to the external circuit makes the interfacial reactions more complicated. Even without the participation of active material, the electrochemical reduction or oxidation decomposition of many SSEs is remarkable at the interface with conductive carbon, when the electrode potential is out of the electrochemical window of the SSE. During cycling, the volume change and chemical–mechanical effect cause new interfaces continue to appear, and the

persistent chemical and electrochemical side reactions make the interface resistance increasing and thereby lead to poor cycling stability. To improve the interface compatibility and stability, on one hand, we should promote the inherent chemical and electrochemical stability of the SSE, and choose the most appropriate SSE with required electrochemical window for given cathode and anode; on the other hand, we can introduce the above-mentioned buffer layer and liquid additive as well as protective layer on the active material or SSE particles (by solution immersion,^[61] sol-gel,^[62] ALD/MLD,^[62] etc.) as interlayer with high compatibility to both of the SSE and active material.

3.3. Fabrication methods of SSBs for laboratory research

In contrast to that conventional batteries with liquid electrolytes have mature fabrication processes for either laboratory research or industrial manufacture, there lacks uniform standards for the electrode composition and cell fabrication of SSBs at present. However, they have significant impacts on the electrochemical performance, and inappropriate composition and fabrication may even mislead us to incorrectly evaluate the

performance and understand the mechanism of the battery system. For example, even for the measurements of ionic conductivity and electrochemical window of a specified SSE, there is usually remarkable difference among the results in different reports. As a rough guide, in Figure 4 we summarize the two typical methods used to fabricate SSBs in laboratory, namely coin cells and mould cells (punch cells have been also reported but are much less popular). It is worth noting that in different reports the detailed procedures may be a little different, and sometimes special processes may be applied to improve the battery performance.^[63]

Coin cells have been widely used to study common battery systems with liquid and gel electrolytes, and they can be also applied to investigate SSBs with SPEs, SCEs, and oxide-type SIEs (Figure 4a). The preparation of the electrolyte layer is quite different for different kinds of SSEs and thus will not be discussed herein (it can be found in the research works focusing on that type of SSEs). In terms of SPEs and SCEs, the cathode composition and cell assembly are very similar to those for liquid and gel electrolytes. The cathode disks are prepared by mixing the active material, conductive carbon, and binder into a viscous slurry, coating the slurry onto a current collector (e.g., Al foil), drying, and punching. For ion con-

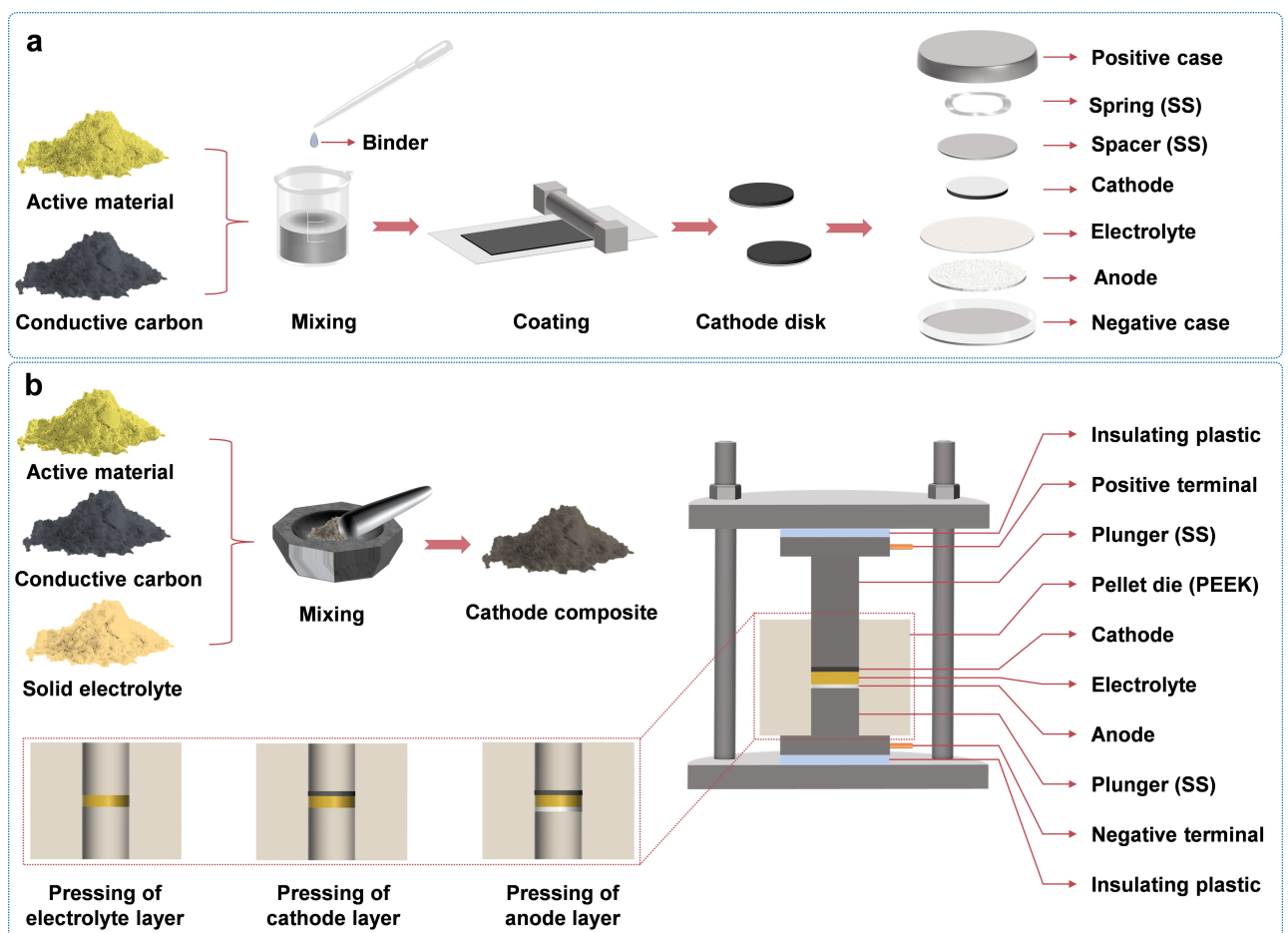


Figure 4. Typical fabrication processes and cell configurations of solid-state batteries for laboratory research: a) coin cells using SPEs and SCEs; b) Mould cells using SIEs.

duction inside the cathode layer, it is possible for the polymer electrolyte permeating into the cathode under certain pressure (maintained by the spring in the coin cell) and heating temperature (in the treatment after cell assembly or during battery testing). Usually, a certain amount of polymer electrolyte can be also added into the cathode composite to enhance the ion conduction and take the place of binder. It is also widely used for oxide-type SIEs with high rigidity, because they can hardly form good physical contact with active material in the cathode through ordinary methods, or permeate into the cathode layer after cell assembly.

In terms of sulfide and halide electrolytes with much higher flexibility than oxide electrolytes, the electrolyte layer can be prepared just by cold or hot pressing rather than sintering. Therefore, SSBs based on them are mainly fabricated by using a special mould consisting of a plastic [e.g., polyetheretherketone (PEEK)] die, two metal (e.g., stainless steel (SS) or Ti) plungers, and an external fixture (Figure 4b). The typical fabrication process contains four steps: 1) the electrolyte powder is compressed into a pellet in the die under a pressure of 150–200 MPa by a tablet compressing machine; 2) the active material, conductive carbon, and SSE are well mixed by grinding or ball milling, and the obtained cathode composite is uniformly distributed on one side of the electrolyte pellet, and pressed under a pressure of 150–400 MPa for several minutes; 3) the anode (e.g., Li and Na foils, and InLi and SnNa alloys) is added to the other side of the electrolyte pellet, and pressed under a pressure of 150–200 MPa; 4) the assembled mould cell with the two plungers as current collectors is fixed in the fixture, which provides a certain external pressure (typically

0.5 MPa, which can be monitored through a pressure sensor) by adjusting the tightness of the screws. To avoid deliquesce and side reactions with air, the whole process need to be conducted in a glove box filled with inert gas, and the whole device needs to be stored also in the glove box or a sealed bag during electrochemical testing.

4. Solid-State Batteries (SSBs) based on Organic Cathode Materials (OCMs)

From Section 2 and 3, we can have a basic understanding of the advantages and problems of OCMs and SSBs, respectively. Obviously, it is a fundamental solution for OCMs to replace conventional liquid electrolytes by SSEs. It cannot only totally solve the dissolution problem and shuttle effect of organic cathodes, but also inhibit the growth and penetration of Li and Na metal anodes, resulting in higher cycling stability, Coulombic efficiency, and safety (Figure 5). Meanwhile, the high theoretical energy density, good flexibility, and moderate redox potential of OCMs also provide SSBs new opportunities to improve the electrochemical performance. Moreover, the non-mobility of SSEs endows the possibilities of bipolar electrode design and inner series connection of batteries, which can further increase the energy density by reducing the use of package and tap materials.^[50a] Briefly, the combination of OCMs and SSB is an excellent strategy to kill many birds with one stone and an important research orientation towards the practical application of them.

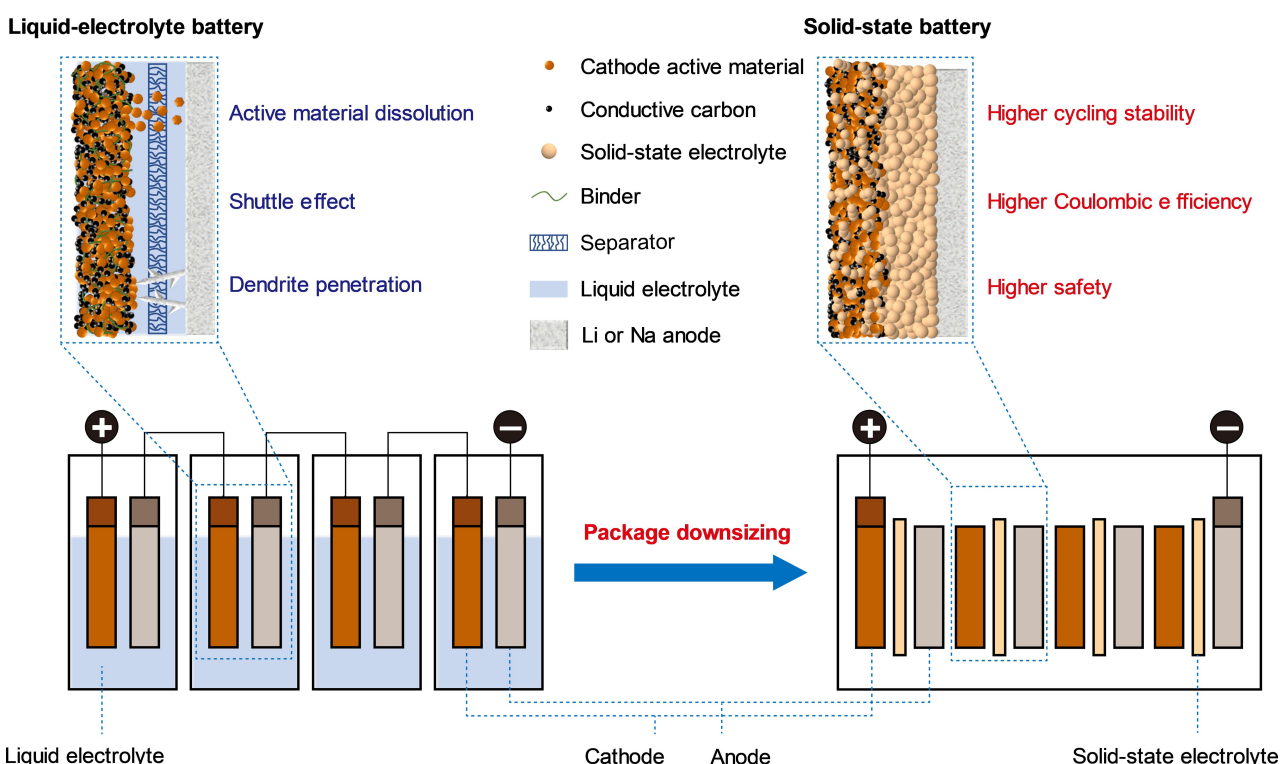


Figure 5. Advantages of solid-state batteries over liquid-electrolyte batteries based on organic cathode materials (OCMs).

The choice of SSE greatly determines the choices of OCM and anode, cathode composition, cell fabrication, working temperature, and electrochemical performance. For SIEs with cation transference number of nearly 1, obviously only n-type OCMs can be employed, and thus the anode must be metal or alloy as the source of Li^+ or Na^+ ion. For SPEs and SCEs with both cations and anions as mobile ions, either n-type or p-type OCMs are applicable, but the latter ones receive much less attention. In the subsequent sections, the SSBs based on OCMs so far reported are categorized into non-ceramic, semi-ceramic, and all-ceramic ones. They are roughly consistent with the above classifications of SSEs (i.e., SPE, SCE, and SIE), but some special SSEs are also involved, especially for the non-ceramic ones.

4.1. Non-ceramic SSBs based on OCMs

Figure 6 presents the schematic of a typical punch cell of non-ceramic SSBs, which is mainly comprised of cathode composite (containing OCM, conductive carbon, and SPE that also plays the role of binder), SPE, and Li foil anode. The most popular SPE is the LiTFSI–PEO system (PEO can be derived into various copolymers), which can only achieve a required ion conductivity ($10^{-3} \text{ S cm}^{-1}$) at relatively higher temperature (e.g., above 60°C). Although elevating working temperature is also beneficial to reduce the interface resistance and promote the redox reaction kinetics, it is an obvious disadvantage for practical application and addressing the dissolution problem of OCMs.

In fact, the earliest report on SSBs based on OCMs can be traced back to 1991, when Liu et al.^[64] investigated a series of organodisulfide cathodes [including PDMcT and poly(trithiocyanuric acid) (PTTCA)] with the LiTFSI–PEO electrolyte. However, to achieve acceptable electrochemical performance, the testing temperature was set at $60\text{--}100^\circ\text{C}$, at which the polymer electrolyte is in a molten and highly viscous state that can hardly prevent the dissolution of those organo-disulfides (especially after breaking the S–S bonds in discharge process). In recent years, Lécyer et al. tested the electrochemical performance of carbonyl-type OCMs including tetramethoxy-p-benzoquinone (TMQ)^[29] and indigo carmine

(IC)^[65] with the LiTFSI–PEO electrolyte under 100°C . In spite that their theoretical capacities were approximately fully realized and the shuttle effect was inhibited, the cycling stability was still unsatisfactory because of the dissolution and diffusion of active material in the polymer electrolyte at such a high temperature. In summary, the LiTFSI–PEO electrolyte is more like a gel electrolyte or high-viscosity liquid electrolyte at higher temperature, which have compromised ability to prevent the dissolution and diffusion of OCMs, especially considering their increased volatility at elevated temperature.

Besides PEO, PPC is another commonly used polymer to construct SPE. Fei et al.^[25b] prepared a NaFSI–PPC–cellulose-nonwoven composite electrolyte, and employed it to tested PTCDA as a cathode for SSSB. Despite the reduced reversible capacity, the cycling stability of PTCDA at RT was greatly improved compared to that in liquid carbonate-ester-based electrolyte. However, it is worth noting that PPC is relatively unstable and may be decomposed to produce liquid components in electrolyte preparation and battery testing processes, which significantly improves the ionic conductivity and thus makes the SSB working at RT possible.^[66]

In addition to the above typical SPEs composed of neutral polymer and alkali metal salt, polyelectrolytes composed of positive- or negative-charged polymer chain and counterions have been also applied in non-ceramic SSBs based on OCMs. Generally, according to the types of polyelectrolytes, there are three different ways to design the battery (Figure 7). The first type is single-cation conducting polyelectrolytes comprised of anodic polymer chains and mobile cations such as Li^+ and Na^+ ions, which are mainly applied for n-type OCMs matched with alkali metal anodes. The electrostatic repulsion effect of the anodic polymer chains is useful to prevent the negative-charged reduction products of the OCM from diffusing in the electrolyte. For example, Kim et al.^[67] prepared a TFSI-functionalized polystyrene nanoparticle electrolyte with a Li^+ ion transference number of 0.99, and employed it to test the electrochemical performance of poly(4-vinylcatechol) (P4VC). Unfortunately, because of the dissolution of partial P4VC with relatively low molecular weights into the residual SCN solvent in the electrolyte, the capacity retention after 100 cycles was only 51%. Li et al.^[68] synthesized a covalent organic framework (COF) and functionized it with different groups including carboxylate, phenolate, and sulfonate. The sulfonate-based LiCON-3 electrolyte demonstrated the highest ionic conductivity of $3.2 \times 10^{-5} \text{ S cm}^{-1}$ at 20°C and a Li^+ ion transference number of 0.92. Due to the insufficient ionic conductivity, LiCON-3 was mixed with LiTFSI-SCN plastic crystal to form a quasi-solid electrolyte, with which BQ achieved stable cycling over 500 cycles with a capacity of about 200 mAh g^{-1} . However, it is worth noting that the mass loading of BQ is only 0.05 mg cm^{-2} , which is too low to accurately evaluate the effect of the electrolyte.

The second type is single-anion conducting polyelectrolytes comprised of cationic polymer chains and mobile anions such as TFSI^- ions, which are also known as cationic poly(ionic liquid)s (PILs). They can be applied in the unusual anion rocking-chair batteries using p-type electroactive organics as

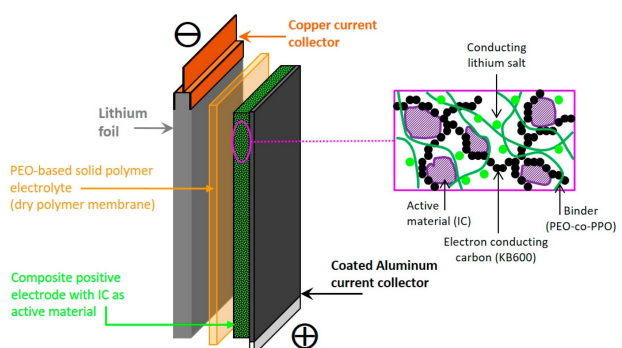


Figure 6. Schematic of a typical punch cell of non-ceramic SSBs. Adapted with permission from Ref. [65]. Copyright (2020) The Author(s). Published by MDPI.

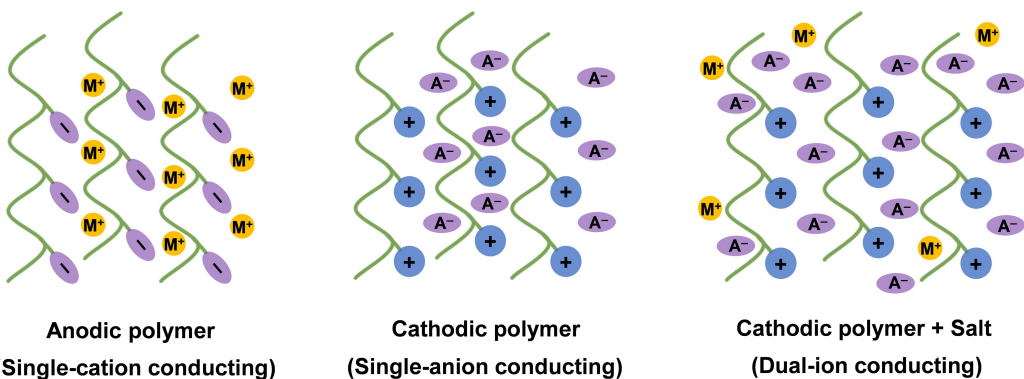


Figure 7. Schematic of three types of polyelectrolyte-based SPEs.

both cathode and anode. For example, Hatakeyama-Sato et al.^[69] reported a thin-film battery with a thickness of merely 2 μm , consisting of polyethers substituted by TEMPO, imidazolium, and viologen as cathode, electrolyte, and anode, respectively, all of which have the same anion of TFSI^- . Despite the low energy density, this work exhibited the application prospects of OCM-based SSBs in flexible, wearable, and printable devices.

The third type is composed of PIL and alkali metal salt (usually with the same anion as the PIL) dissolved in it, which is a conductor for both metal cation and anion. They can be used in dual-ion batteries consisting of p-type organic cathode and metal or n-type organic anode. For example, Leung et al.^[70] reported a symmetric all-organic SSB fabricated by spray printing method, with such a kind of electrolyte and a commercial dye, i.e., dispersed blue 134 (DB), as both cathode and anode. DB is a bipolar-type organic molecule with n-type anthraquinone and p-type amine moieties, which enables the design of symmetric dual-ion battery. In spite of the relatively low voltage (1.2 V) and reversible capacity (80 mAh g^{-1}), it provides a new idea to prepare all-organic flexible batteries.

As a summary of non-ceramic SSBs with OCMs, there is a dilemma for this system. On one hand, the ionic conductivities of SPEs are too low for the SSB to work at RT, so it is necessary to elevate the working temperature or make the SPE containing more or less liquid component (e.g., residual solvent, melted plastic crystal, ionic liquid) to reach an acceptable ionic conductivity at RT. On the other hand, either of the above methods is adverse to inhabitation of the dissolution of OCMs, especially SMOCMs, and thereby always results in poor cycling performance. To overcome this dilemma, maybe it is a good choice to develop flexible thin-film batteries based on SPEs and OCMs, which can reduce the requirement on ionic conductivity and give full play to their advantages of high flexibility and processability.

4.2. Semi-ceramic SSBs based on OCMs

To enhance the ionic conductivity and mechanical strength of SPEs (especially, the most popular LiTFSI-PEO electrolyte), various inorganic fillers including inert ones (e.g., Al_2O_3 , SiO_2 ,

TiO_2 , and ZrO_2) and ionic conductors (e.g., LAGP, LLZO, and LLZTO) have been added to form SCEs. However, maybe due to the difficulty of fabricating a high-performance SCE containing SIE, such kinds of “ceramic in polymer” or “polymer in ceramic” electrolytes have not been applied for OCMs yet. Adopting inert nanofillers is much easier but also effective to improve the electrochemical performance of SSBs based on OCMs.

Zhu et al.^[71] compared the ionic conductivities of a series of SCEs based on PMA- LiClO_4 and PMA-PEG- LiClO_4 systems and different addition amounts of SiO_2 and TiO_2 nanofillers, and finally chose PMA-PEG- LiClO_4 - SiO_2 (3 wt%) as the optimized one with the highest ionic conductivity of 0.26 mS cm^{-1} at RT. By using this electrolyte, they tested the pillar[5]quinone (P5Q) cathode at RT and achieved excellent electrochemical performance including an average operation voltage of 2.6 V, an initial capacity as high as 418 mAh g^{-1} , and 95% capacity retention after 50 cycles (Figure 8). Since such kind of SCEs have similar properties to the base SPEs including the conductivity for both cation and anion, they can be also used for p-type OCMs. For example, Wu et al.^[73] employed LiTFSI-PEO-Gd_{0.1}Ce_{0.9}O_{1.95} (5 wt %) as an optimized SCE (with an ionic conductivity of $10^{-4} \text{ mS cm}^{-1}$ at 35°C) to test the electrochemical performance of the most famous p-type OCM, i.e., PAni. At a testing temperature of 35°C , it delivered a reversible capacity of 110 mAh g^{-1} and stable cycling over 150 cycles.

Another type of semi-ceramic SSBs is that using a SIE as the electrolyte layer but a SPE in the cathode composite, which can not only enhance the internal physical contact and ionic conduction (sometimes also plays the role of binder), but also reduce the interface resistance between the cathode and electrolyte layers. As shown in Figure 9, Chi et al.^[72] constructed a SSSB by using PTO as the OCM, NaClO₄-PEO as the SPE in cathode, β -Al₂O₃ (BASE) as the electrolyte layer, Na metal as the anode, and a Sn thin film as the buffer layer between the electrolyte and anode layers. At a working temperature of 60°C , PTO delivered a high initial discharge capacity of 358 mAh g^{-1} (corresponding to 88% of its theoretical capacity) and a capacity retention of 80% after 50 cycles. Similarly to the non-ceramic SSBs with only SPEs, the slow dissolution and diffusion of the OCM still occur in the cathode. The advantages of using SIE to replace SPE as the electrolyte layer, need to be further proved in the future. Especially, the 1–2 orders of

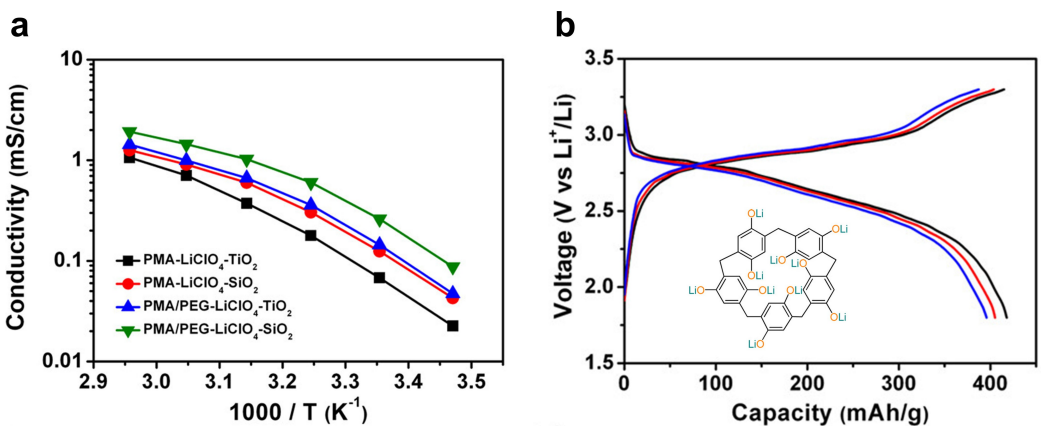


Figure 8. Information of the semi-ceramic Li-P5Q battery based on SCE (PMA/PEG-LiClO₄-SiO₂): a) ionic conductivities of electrolytes with different compositions; b) discharge-charge curves at different cycle numbers (1.8–3.3 V, 82 mA g⁻¹, 25 °C) with inset showing the structure of P5Q. Reproduced with permission from Ref. [71]. Copyright (2014) American Chemical Society.

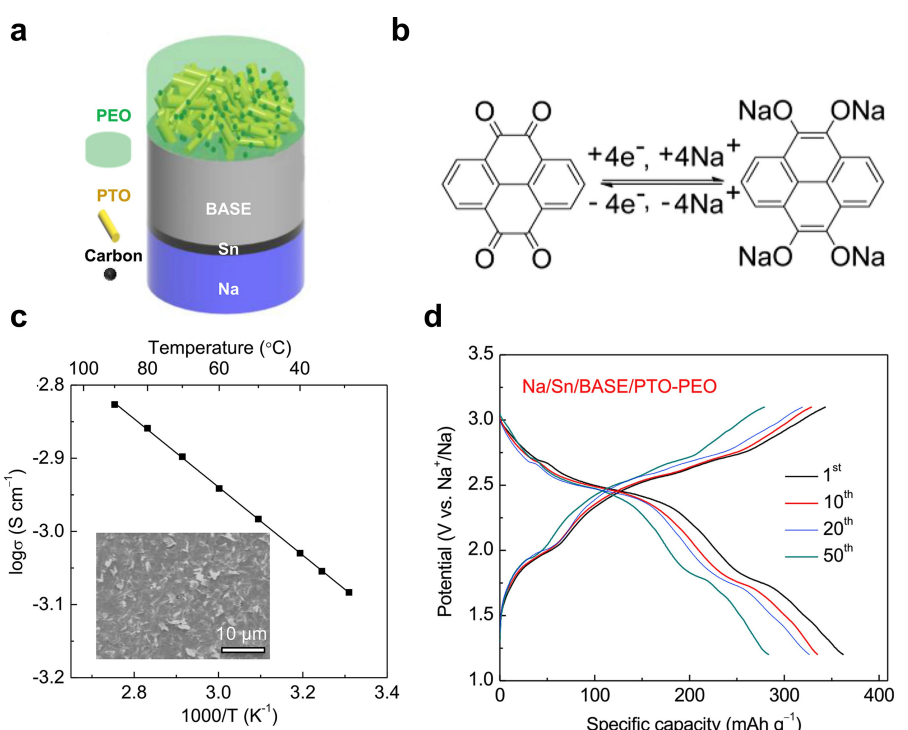


Figure 9. Information of the semi-ceramic Na-PTO battery based on β-Al₂O₃ (BASE) and NaClO₄-PEO electrolytes: a) Schematic of the cell; and b) electrochemical redox mechanism; c) Arrhenius plot of ionic conductivity and cross-sectional scanning electron microscopy (SEM) image of BASE; d) discharge-charge curves at different cycle numbers (1.2–3.2 V, 41 mA g⁻¹, 60 °C). Reproduced with permission from Ref. [72]. Copyright (2019) Elsevier.

magnitudes higher ionic conductivity may lower down the working temperature.

4.3. All-ceramic SSBs based on OCMs

With either SPE or SCE, the indispensable segmental motion of the polymer chain makes the dissolution issue of OCMs still existing. To fully address it, all-ceramic SSBs using only non-mobile SIEs are obviously more appropriate. Due to the cation transference number of close to 1, only n-type OCMs can match

with SIEs to assemble the battery. For oxide-type SIEs with high rigidity, it is always necessary to use a co-sintering method to prepare the cathode layer with high integrity and low interface resistance, which is applicable for inorganic cathode materials but unapplicable for OCMs with much poorer thermal stability.

Therefore, although so many high-performance oxide electrolytes have been reported, they have been barely used for OCMs. In addition, the newly developed halide electrolytes have not attracted the attention in this field yet. The all-ceramic SSBs based on OCMs so far reported mostly employ sulfide

electrolytes, except for one work using LiPON to construct thin-film batteries.

Nisula et al.^[31] fabricated thin-film batteries by ALD/MLD technique, which were composed of a 5–42 nm layer of lithiated p-benzoquinone (Li_2Q) cathode and a 30 nm layer of LiPON electrolyte (Figure 10). Because that the as-prepared cathode is in an unusual lithiated state, an anode-free design was able to be realized, and dilithium terephthalate (Li_2TP) was also introduced to construct an all-organic all-solid thin-film battery. Due to the absence of SSE in the cathode layer, the utilization of the OCM was highly depended on its thickness. It was found that the areal capacity no longer increased with the thickness if it was larger than 10 nm.

Sulfide electrolytes have superior ionic conductivity and high flexibility, and can be easily made into pellets by cold or hot compression, with or without the addition of cathode active material and conductive carbon. Therefore, they have been intensively used to fabricate SSBs based on OCMs. One obvious shortcoming of sulfide electrolytes is the narrow electrochemical window. On the anode side, because of the poor chemical compatibility of them with Li and Na metal anodes, an alloy anode with higher and constant redox potential (e.g. InLi at 0.6 V vs. Li^+/Li and SnNa at 0.2 V vs. Na^+/Na) is usually used as an alternative, or a buffer layer has to be introduced to enable the use of the metal anode. On the cathode side, because of the easy oxidation decomposition of sulfide electrolytes, the cathode potential is preferred to be no higher than 3.5 V vs. Li^+/Li , so they are incompatible with most inorganic cathode materials but compatible with most n-type OCMs. In 2018, Luo et al.^[75] reported the first all-solid-state lithium-organic battery based on sulfide electrolyte, featuring with 4-(phenylazo) benzoic acid lithium salt (PBALS) as the OCM and Li_3PS_4 as the electrolyte. The authors claimed that the interaction between the lithium carboxylate group of PBALS

and Li_3PS_4 facilitated the uniform dispersion of PBALS in the cathode and its intimate contact with the electrolyte. At RT, it realized relatively stable cycling but the low reversible capacity (128 mAh g^{-1}) and discharge voltage (averagely 1.3 V) reduced its competitiveness. Yang et al.^[76] synthesized A truxenone-based COF (COF-TRO) and tested it as cathode with argyrodite electrolyte. Although both high reversible capacity (268 mAh g^{-1}) and high cycling stability within 100 cycles were achieved, the poor reversibility of discharge-charge curves at 60°C confused the understanding of the redox reaction mechanism.

The cathode composition and structure have a crucial influence on the electrochemical performance of SSBs including those based on sulfide electrolytes and OCMs. In this respect, the Yao group^[78] has reported a series of works on PTO cathode material with sulfide electrolytes (all the electrochemical tests were conducted at 60°C) to reveal the effects of different electrode fabrication methods and component weight ratios (OCM/SSE/C).

High-energy ball-milling is a commonly used method to reduce the particle size and improve the uniform mixing of active material and SSE. However, due to the relatively low mechanical stiffness of either OCMs or sulfide electrolytes, it is usually less effective to make them into a homogeneous mixture. Especially, the increased temperature caused by ball-milling further reduces the stiffness and facilitate the aggregation of OCM particles. Therefore, the authors employed a cryomilling technique to keep the brittleness and prepared a homogeneous composite (PTO/ $\text{Li}_3\text{PS}_4/\text{C} = 20:70:10$), in which the sizes of PTO domains were about one order of magnitude smaller than those using hand-milling (Figure 11a,b).^[74] Consequently, the theoretical capacity of PTO (409 mAh g^{-1}) was fully realized (Figure 11c, d). In addition to the cryomilling method, they also used a solvent-assisted grinding procedure

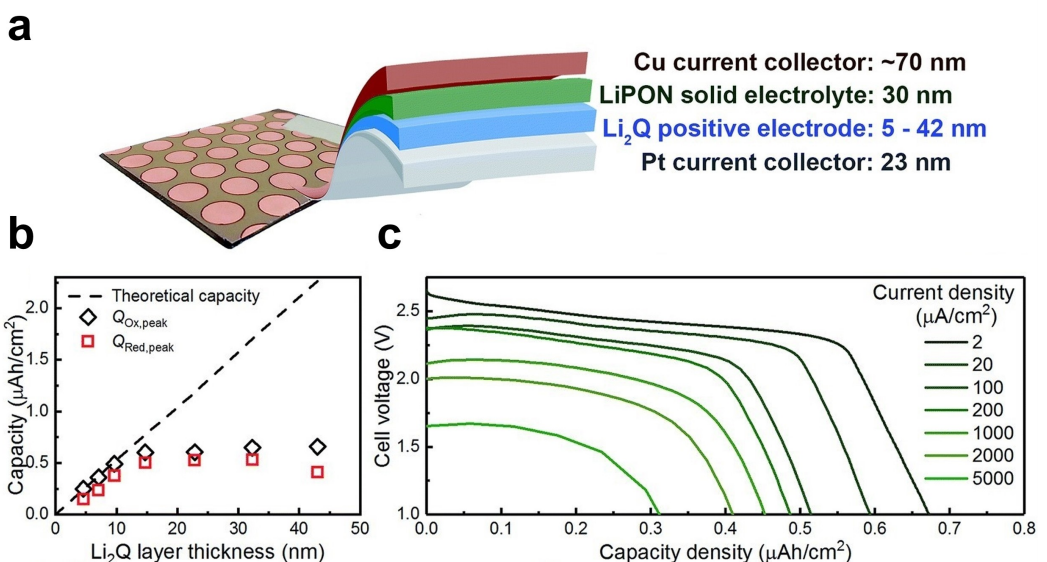


Figure 10. Information of the anode-free thin-film SSB based on Li_2Q cathode and LiPON electrolyte: a) schematic of the thin-film cell; b) the relation between capacity and Li_2Q layer thickness; c) discharge curves under different current densities ($2\text{--}5000 \text{ mA cm}^{-2}$, equivalent to $2.6\text{--}6500 \text{ C}$) at a Li_2Q layer thickness of 15 nm. Adopted with permission from Ref. [31]. Copyright (2018) The Royal Society of Chemistry.

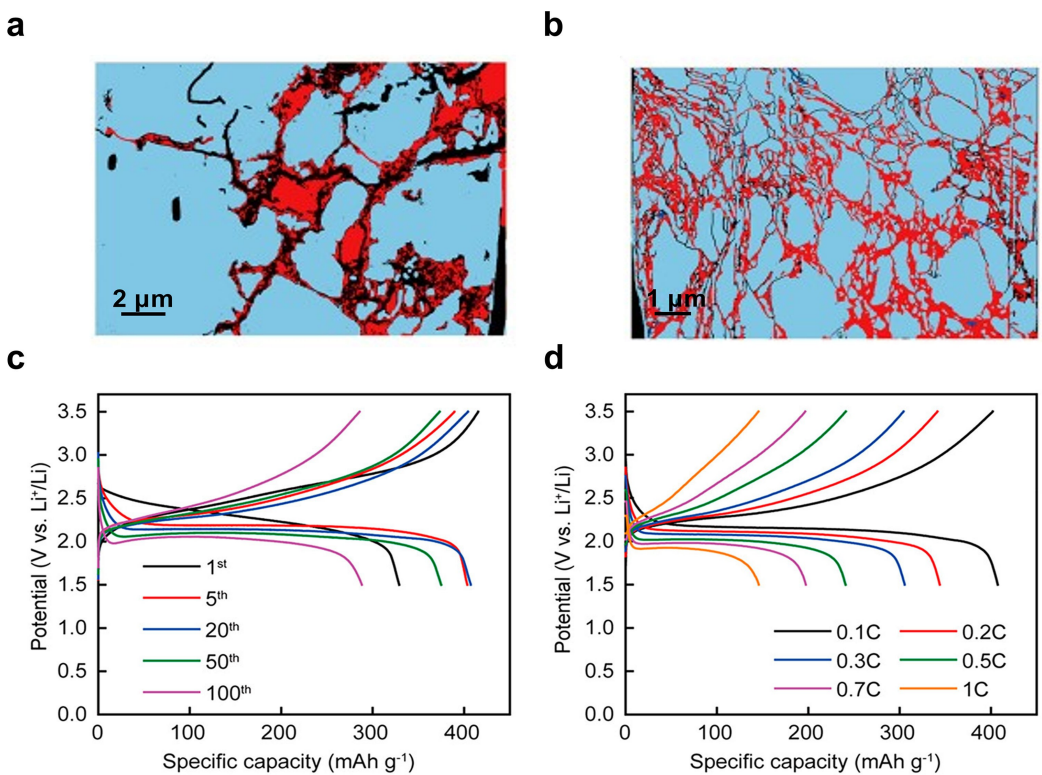


Figure 11. Information of the all-ceramic Li-PTO battery based on sulfide electrolyte (Li_3PS_4): a, b) segmented binary SEM images (red for PTO and blue for Li_3PS_4) of the cathode composites prepared by a) hand-milling and b) cryomilling; c, d) discharge-charge curves at c) different cycle numbers (at 0.1 C) and d) different current rates (1.5–3.5 V, 60 °C). Reproduced with permission from Ref. [74]. Copyright (2021) American Chemical Society.

to optimize the microstructures of the cathode composite containing different contents (20–50 wt%) of PTO. By using ethanol as a solvent that can dissolve the $\text{Li}_6\text{PS}_5\text{Cl}$ electrolyte, a uniform distribution of PTO was maintained at a weight ratio of 40 wt%, leading to a high capacity utilization of 98%.^[78c] It is worth noting that polar solvents including ethanol also cause partial decomposition of the sulfide electrolytes, and thus have adverse impact on the interfacial impedance.

Besides the mixing of OCM and SSE, the kind, proportion, and distribution of conductive carbon in the cathode composite are also very crucial. The Yao group^[78b] investigated the influence of different weight ratios of carbon ($x=0, 5, 10, 20, 27$, and 33 wt%) in the cathode composite [$\text{PTO}/\text{Na}_3\text{PS}_4/\text{C}=20:(80-x):x$] on the electrochemical performance. The best ratio was found to be 10 wt%, because the conductive carbon provided insufficient electron conduction for the redox reaction of the OCM at lower ratios, but caused severe electrochemical oxidation decomposition of the sulfide electrolyte at higher ratios. Moreover, it was also found that the decomposition products of the sulfide electrolyte also showed partial redox reversibility and could contribute considerable capacity. In addition to the weight ratio, Zhou et al.^[79] investigated the influence of various conductive carbons with different specific surfaces (VGCF, Super P, and KB), by using 5,7,12,14-pentacenetetrone (PT) as the OCM and $\text{Li}_2\text{P}_3\text{S}_{11}$ as the electrolyte. Super P with moderate specific surface was found to be the best choice, due to the similar reason as discussed above.

In addition to the above concerns, the chemical compatibility between the OCM and sulfide electrolyte is another important factor affecting the electrochemical performance, especially for the intensively studied carbonyl-based OCMs. Ji et al.^[77] investigated the chemical compatibility of $\text{Li}_6\text{PS}_5\text{Cl}$ with three typical quinone-type cathode materials including BQ, AQ, and poly(anthraquinonyl sulfide) (PAQS). It was found that there is a nucleophilic side reaction between them and the reactivity order was $\text{BQ} \gg \text{AQ} > \text{PAQS}$ (Figure 12a). It is reasonable because the reactivity is mainly determined by the oxidizing ability of the OCM and the contact area between the OCM and the sulfide electrolyte. Finally, they prepared a PAQS-graphene composite for enhanced electron conduction, and tested it as a cathode for both SSLBs and SSSBs (using $\text{Li}_6\text{PS}_5\text{Cl}$ and Na_3PS_4 as the electrolytes, respectively). At 60 °C, both batteries exhibited a reversible capacity of about 180 mAh g^{-1} (corresponding to a utilization of 80%) and a high cycling stability (within 200 or 300 cycles) (Figure 11b, c).

For all the above examples of carbonyl-based OCMs tested with sulfide electrolytes, the presented electrochemical performance was obtained at 60 °C rather than RT. Since the RT ionic conductivities of the used sulfide electrolytes ($> 10^{-3} \text{ Scm}^{-1}$) are high enough, and the interface physical contact has been proved not a big problem, the barrier is probably the chemical and electrochemical compatibilities between them. Yang et al.^[32] explained it based on the hard and soft acid and bases (HSAB) theory: as a hard base, O of H_2O preferentially attacks the hard acid P of sulfide electrolyte and

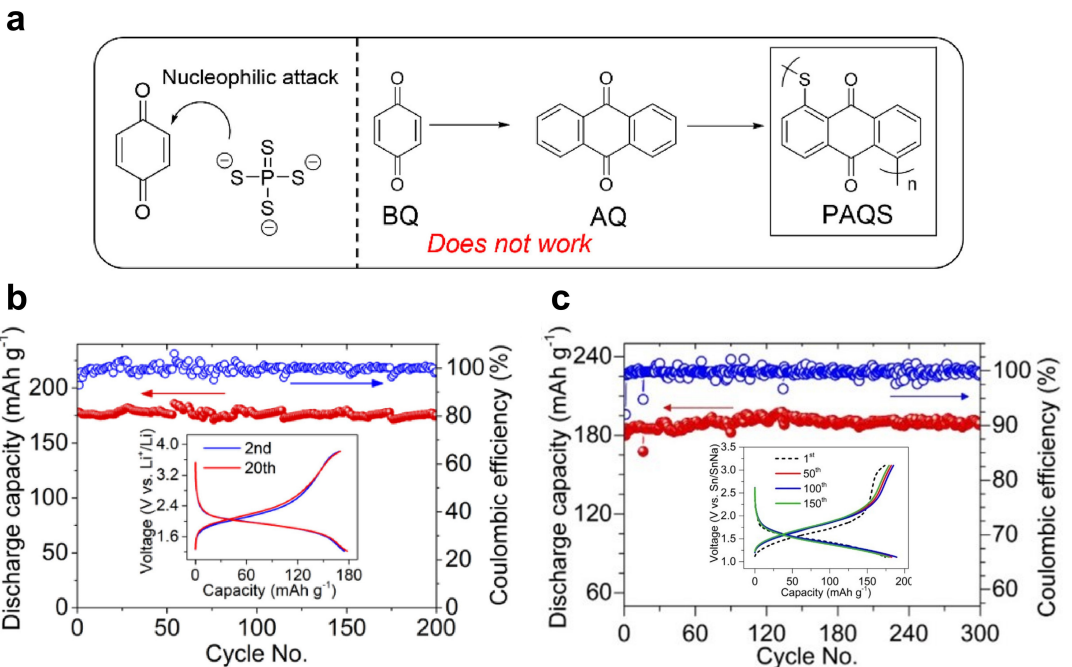


Figure 12. a) Proposed side reaction between BQ cathode and sulfide electrolyte, and the corresponding optimization of active material. b, c) Cycling performance and the corresponding discharge-charge curves (18 mA g^{-1} , 60°C) of the all-ceramic b) Li-PAQS-G battery based on $\text{Li}_6\text{PS}_5\text{Cl}$ electrolyte and c) Na-PAQS-G battery based on Na_3PS_4 electrolyte. Reproduced with permission from Ref. [77]. Copyright (2022) Elsevier.

replace the soft base S, which has been proved by the easy deliquescence of sulfide electrolytes; similarly, the hard base O of carbonyl in discharged state ($\text{C}-\text{O}^-$) may also interact with the hard acid P, which hinders its recharge reaction to carbonyl. In this context, they proposed that organodisulfides with “softer” S–S bonds are more compatible, and realized the first room-temperature SSB based on sulfide electrolytes and OCMs

(Figure 13). The combination of PTTCA/CNT composite cathode and $\text{Li}_3\text{P}_3\text{S}_{11}$ electrolyte provided enhanced electron conductivity and electrochemically favorable interfaces, and thus realized excellent electrochemical performance at RT, including a reversible capacity of 410 mAh g^{-1} (corresponding to a utilization of 91%), an energy density of 767 Wh kg^{-1} , and a capacity retention of 83% after 100 cycles. The comparison study

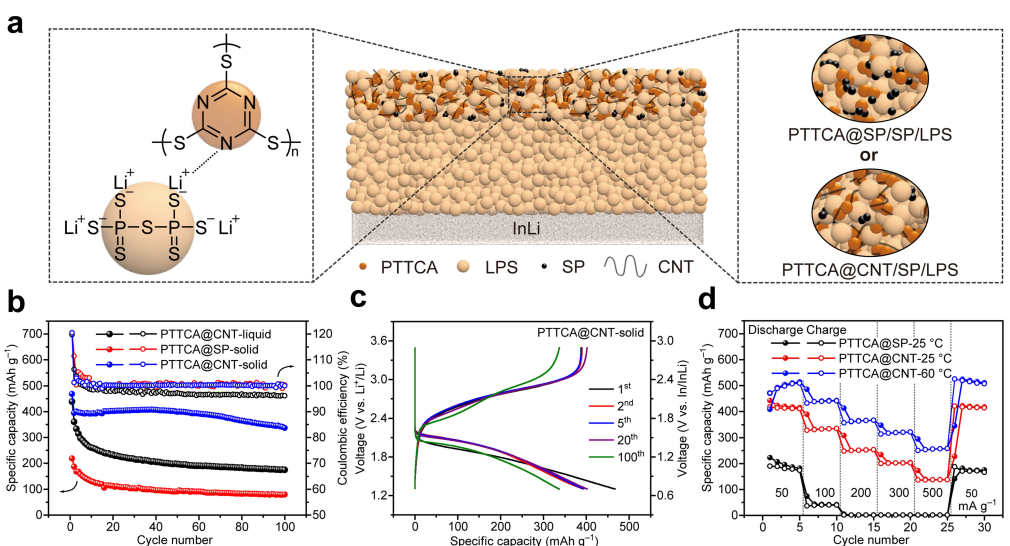


Figure 13. Information of the all-ceramic Li-PTTCA batteries based on sulfide electrolyte ($\text{Li}_3\text{P}_3\text{S}_{11}$): a) schematic of the cell and the internal chemical interaction between $\text{Li}_3\text{P}_3\text{S}_{11}$ and PTTCA; b) cycling performance of PTTCA@SP and PTTCA@CNT composites in the liquid-electrolyte and all-solid-state cells (1.3 – 3.5 V, 50 mA g^{-1} , 25°C) and c) the corresponding discharge-charge curves of PTTCA@CNT in the all-solid-state cell; d) rate performance of PTTCA@SP and PTTCA@CNT composites in the all-solid-state cells at different temperatures (25 and 60°C). Reproduced with permission from Ref. [32]. Copyright (2021) John Wiley & Sons.

between PTTCA and PAQS further verified the superiority of organodisulfides over carbonyl compounds in this system. Subsequently, Ji et al.^[80] also demonstrated the excellent battery performance at RT of a thiuram polysulfide, namely dipentamethylenethiuram hexasulfide (PMTH), as a cathode for both SSLBs and SSSBs (using Li₆PS₅Cl and Na₃PS₄ as the electrolytes, respectively).^[80] The high theoretical capacity of PMTH (597 mAh g⁻¹) was fully realized at either 25 or 60°C, in either Li or Na batteries, and the cycling was also quite stable within hundreds of cycles under different conditions. It once again proved the advantage of organosulfur cathode materials for SSBs using sulfide electrolytes.

5. Conclusions and Outlook

In Table 2, we summarize the battery configurations and electrochemical performance of almost all the reported SSLBs and SSSBs based on OCMs. Generally, the most favorable SSEs are the LiTFSI–PEO electrolytes and sulfide electrolytes, while the most intensively investigated OCM are carbonyl-based ones. These reports have already exhibited the effect of SSEs to address the dissolution problem and shuttle effect of OCMs. However, the capacity utilization, voltage polarization, cycling stability, and rate capability still have a large room for improvement. Towards practical application, the weight ratio and loading of OCM in the cathode composite should be significantly improved, and the thickness of electrolyte and anode layers should be greatly reduced. Since the research in this field is still in its infant stage, the influences of various factors on the electrochemical performance are still unclear. To uncover the influence rules and the mechanisms behind them, we need more systematic investigations and strict single factor experiments. In the following paragraphs, we venture to conclude our understandings on the main scientific issues and possible solutions of SSBs based on OCMs.

1) Choice of SSE. Different types of SSEs have different advantages and disadvantages, and the inherent drawbacks are always very difficult to overcome, or can be overcome through complicated and costly procedures. Therefore, it is suggested to choose the SSE satisfying the most emphasized parameter for the specific goal on electrochemical performance. For example, if requiring the SSB to work at RT, sulfide and halide electrolytes with the highest ionic conductivity are the most appropriate choice at present, in spite of their poorer chemical stability and limited electrochemical window. If the working temperature can be elevated to about 40 and 60°C, SCEs and SPEs with much poorer ionic conductivities are also applicable, respectively. However, it should be noted that their effect on preventing the dissolution of OCMs is much weaker than SIEs and may be similar to high-viscosity liquid electrolytes, especially at higher temperature. For oxide electrolytes, it is difficult for them to form intimate contact with OCMs in the cathode layer, so they can be only applied as the electrolyte layer and used together with another SSE in the cathode.

- 2) Matching between OCM and SSE. Different kinds of OCMs can be matched with different types of SSEs. For example, p-type OCMs (e.g., PAni) can only work at relatively high temperature with SPEs and SCEs, which have both cations and anions as mobile ions as well as high-potential stability. In theory, n-type OCMs including carbonyl, imine, organodisulfide, and azo compounds can be matched with all the above-mentioned SSEs including SPEs, SCEs, and SIEs. However, in addition to the working temperature, two crucial issues should be concerned, which will be discussed in the next two paragraphs.
- 3) Ion diffusion in OCM particles. In contrast to inorganic cathode materials with known pathways and sufficient coefficients of ionic diffusion, it is still ambiguous whether the ion can diffuse in the crystalline particles of OCMs at a required rate, which is paid little attention in the past research. It is not a big problem in conventional batteries using liquid electrolytes, in which the SMOCMs are more or less dissolved and the polymer cathode materials are sufficiently infiltrated. The unavoidable dissolution is actually a double-edged sword, which is harmful to the cycling stability but is beneficial to the ionic conduction because of the significantly reduced particle sizes and increased particle surfaces (moreover, the dissolved species can play the role of redox mediator and facilitate electron transfer). However, in SSBs aiming to completely prevent the dissolution, especially those with highly crystalline SMOCMs and working at RT, the sluggish ionic diffusion in the crystals may be the rate determining step and lead to poor redox kinetics. One possible solution is to mix the OCM and SSE at a much smaller size level (e.g., tens of nanometers), however, which is difficult to realize and may further increase the unfavorable side reactions at the interface.
- 4) Chemical and electrochemical compatibility between OCM and SSE. The compatibility between the chosen OCM and SSE is mainly determined by their relative oxidation-reduction ability and chemical affinity. For example, the LiTFSI–PEO electrolytes have a similar electrochemical window to that of liquid ether-based electrolytes (0–4 V vs. Li⁺/Li), which is proper for most n-type OCMs. In contrast, the sulfide and halide electrolytes usually begin to be oxidized at 3.5 V vs. Li⁺/Li, and reduced at 1.5 V vs. Li⁺/Li, depending on the chemical composition and testing conditions (especially the electrochemical active area). Such an electrochemical window is usually not wide enough for typical n-type OCMs, especially when taking the remarkable voltage polarization in discharge and charge processes into account. An OCM at too high oxidation or too low reduction states will react with the electrolyte at the contact interface. The instability of the interface products during discharge-charge cycling and the continuously generated new interfaces, together cause the deterioration of the electrode structure, which is one of the key reasons of the capacity fading. In addition, if the chemical affinity between the nucleophilic heteroatoms (e.g., N, O, S) of the OCM, especially in discharged state, and the electrophilic atoms

Active material	Cathode composition ^[a]	Solid-state electrolyte ^[b]	Testing temperature	Voltage window and average discharge/charge potential ^[c]	Reversible/theoretical capacity and utilization ^[d]	Cycling performance (reversible capacity @current rate and retention@cycle number) ^[e]	Rate performance (reversible capacity @current rate)	Ref.
TMQ	AM/KB/CNTs/ LiTFSI/PEO = 50:10:8:24	LiTFSI–PEO	100 °C	2.4–3.4 V (vs. Li ⁺ /Li)	216/ 235 mAh g ⁻¹ 92 %	216 mAh g ⁻¹ @235 mAh g ⁻¹ 72%@50 th cycle	—	[29]
IC	AM/KB/ LiTFSI/CPSEB = 70:10:4:16	LiTFSI–PEO	100 °C	1.5–3.2 V (vs. Li ⁺ /Li)	98/115 mAh g ⁻¹ 85 %	98 mAh g ⁻¹ @29 mAh g ⁻¹ 71%@50 th cycle	—	[65]
P4VC	AM/SP/CNTs/PVDF = 30:30:10:30	LiTFSI–SN–PS@PS	25 °C	1.5–4.0 V (vs. Li ⁺ /Li)	269/ 397 mAh g ⁻¹ 68 %	125 mAh g ⁻¹ @794 mAh g ⁻¹ 84%@500 th cycle	269 mAh g ⁻¹ @40 mAh g ⁻¹ 205 mAh g ⁻¹ @80 mAh g ⁻¹ 160 mAh g ⁻¹ @119 mAh g ⁻¹ 135 mAh g ⁻¹ @199 mAh g ⁻¹ 120 mAh g ⁻¹ @397 mAh g ⁻¹	[67]
BQ	AM/KB/SSE = 50:30:20	LiCON ₃	20 °C	1.7–4.0 V (vs. Li ⁺ /Li)	280/ 496 mAh g ⁻¹ 46 %	205 mAh g ⁻¹ @500 mAh g ⁻¹ 88%@500 th cycle	280 mAh g ⁻¹ @250 mAh g ⁻¹ 205 mAh g ⁻¹ @50 mAh g ⁻¹ 100 mAh g ⁻¹ @1000 mAh g ⁻¹	[68]
PTCDA	AM/SP/PVDF = 70/20/10	NaFSI–PPC–cellulose–nonwo- ven	25 °C	1.0–3.0 V (vs. Na ⁺ /Na)	126/ 138 mAh g ⁻¹ 91 %	77 mAh g ⁻¹ @10 mAh g ⁻¹ 99%@50 th cycle	125 mAh g ⁻¹ @20 mAh g ⁻¹ 94 mAh g ⁻¹ @40 mAh g ⁻¹ 57 mAh g ⁻¹ @80 mAh g ⁻¹	[25b]
P5Q	AM/SP/SSSE = 60/20/20	LiTFSI–PVDF–HFP/PEC–LLZO	24 °C	1.5–3.5 V 2.3/2.6 V (vs. Li ⁺ /Li)	122/ 138 mAh g ⁻¹ 88 %	66 mAh g ⁻¹ @10 mAh g ⁻¹ 91%@1000 mAh g ⁻¹	127 mAh g ⁻¹ @10 mAh g ⁻¹ 118 mAh g ⁻¹ @50 mAh g ⁻¹ 114 mAh g ⁻¹ @100 mAh g ⁻¹ 96 mAh g ⁻¹ @300 mAh g ⁻¹	[81]
AQ	AM/PCBS/CNTs/G/ PVDF = 70:10:3:2:10:5	LiClO ₄ –PMA/PEG–SiO ₂	25 °C	1.8–3.3 V 2.6/2.9 V (vs. Li ⁺ /Li)	409/ 446 mAh g ⁻¹ 92 %	409 mAh g ⁻¹ @89 mAh g ⁻¹ 95%@50 th cycle	409 mAh g ⁻¹ @89 mAh g ⁻¹ 361 mAh g ⁻¹ @134 mAh g ⁻¹ 286 mAh g ⁻¹ @223 mAh g ⁻¹ 197 mAh g ⁻¹ @446 mAh g ⁻¹	[71]

Table 2, continued

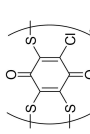
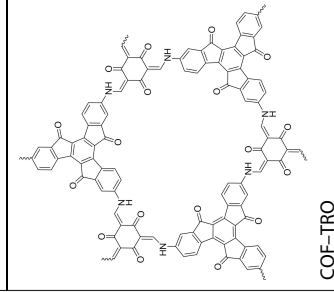
Active material	Cathode composition ^[a]	Solid-state electrolyte ^[b]	Testing temperature	Voltage window and average discharge/charge potential ^[c]	Reversible/theoretical capacity and utilization ^[d]	Cycling performance (reversible capacity @current rate and retention@cycle number) ^[e]	Rate performance (reversible capacity @current rate)	Ref.
TCAQ	AM/SP/PVDF =40:50:10	LiTFSI–PEO–LZTO	25 °C	1.5–3.8 V 2.5/2.8 V (vs. Li ⁺ /Li)	84/176 mAh g ⁻¹ 48%	84 mAh g ⁻¹ @17 mA g ⁻¹ 72%@100 th cycle	–	[30]
PCTB		AM/CC/PVDF =50:30:20	LiClO ₄ –PEO/PEG–LLTO	70 °C	1.6–3.6 V 2.6/2.9 V (vs. Li ⁺ /Li)	104/ 227 mAh g ⁻¹ 46%	104 mAh g ⁻¹ @60 mA g ⁻¹ 90%@300 th cycle	[82]
PAni		AM/CB/LiTFSI/PEO =60:10:10:20	LiTFSI–PEO–Gd _{0.1} Ce _{0.9} O _{1.95}	35 °C	2.0–3.8 V 3.3/3.5 V (vs. Li ⁺ /Li)	110/ 295 mAh g ⁻¹ 46%	110 mAh g ⁻¹ @50 μA cm ⁻² 105 mAh g ⁻¹ @100 μA cm ⁻² 80 mAh g ⁻¹ @200 μA cm ⁻² 50 mAh g ⁻¹ @300 μA cm ⁻²	[73]
Li ₂ Q	AM	LIPON	–	1.0–4.5 V 2.5/3.4 V (vs. Li ⁺ /Li)	380/ 440 mAh g ⁻¹ 87%	380 mAh g ⁻¹ @1136 mA g ⁻¹ 88%@500 th cycle	–	[31]
PBAIS		AM/AB/SSE =25:25:50	Li ₃ PS ₄	25 °C	1.0–1.8 V 1.3/1.5 V (vs. Li ⁺ /Li)	115/ 231 mAh g ⁻¹ 50%	115 mAh g ⁻¹ @41 mA g ⁻¹ 72%@120 th cycle	[75]
COF-TRO		AM/AB/SSE =50:10:40	Argyrodite	60 °C	0.5–4.2 V 1.1/2.1 V (vs. Li ⁺ /Li)	270/ 274 mAh g ⁻¹ 99%	272 mAh g ⁻¹ @27 mA g ⁻¹ 96%@100 th cycle	[76]
Na ₄ C ₆ O ₉	AM/SC65/SSE =40:10:50	Na ₃ PS ₄	60 °C	1.7–2.7 V 2.1/2.3 V (vs. Na ⁺ /Na)	182/ 206 mAh g ⁻¹ 88%	182 mAh g ⁻¹ @20 mA g ⁻¹ 70%@400 th cycle	–	[83]

Table 2, continued

Active material	Cathode composition ^[a]	Solid-state electrolyte ^[b]	Testing temperature	Voltage window and average discharge/charge potential ^[c]	Reversible/theoretical capacity and utilization ^[d]	Cycling performance (reversible capacity @current rate and retention@cycle number) ^[e]	Rate performance (reversible capacity @current rate)	Ref.
AM/CC/SSE = 20:10:70	Li ₃ PS ₄	60 °C	1.5–3.5 V 2.1/2.5 V (vs. Li ⁺ /Li)	407/ 409 mAh g ⁻¹ 100 %	409 mAh g ⁻¹ @41 mAh g ⁻¹ 71%@100 th cycle	409 mAh g ⁻¹ @41 mAh g ⁻¹ 71%@100 th cycle	407 mAh g ⁻¹ @41 mAh g ⁻¹ 344 mAh g ⁻¹ @82 mAh g ⁻¹	[78a]
AM/SP/SSE = 40:10:40	Li ₅ PS ₆ Cl	60 °C	1.5–3.5 V 2.0/2.5 V (vs. Li ⁺ /Li)	411/ 409 mAh g ⁻¹ 102 %	411 mAh g ⁻¹ @41 mAh g ⁻¹ 75%@100 th cycle	411 mAh g ⁻¹ @41 mAh g ⁻¹ 75%@100 th cycle	344 mAh g ⁻¹ @20 mAh g ⁻¹ 397 mAh g ⁻¹ @20 mAh g ⁻¹	[78c]
PTO	β-Al ₂ O ₃	60 °C	1.2–3.2 V 1.9/2.3 V (vs. Na ⁺ /Na)	362/ 409 mAh g ⁻¹ 88 %	362 mAh g ⁻¹ @41 mAh g ⁻¹ 75%@50 th cycle	362 mAh g ⁻¹ @41 mAh g ⁻¹ 75%@50 th cycle	164 mAh g ⁻¹ @123 mAh g ⁻¹ 60 mAh g ⁻¹ @288 mAh g ⁻¹	[72]
AM/SP/PVDF/ NaClO ₄ ·PEO = 30:20:10:40	Na ₃ PS ₄	60 °C	1.1–3.1 V 1.8/2.1 V (vs. Na ⁺ /Na)	322/ 409 mAh g ⁻¹ 79 %	280 mAh g ⁻¹ @123 mAh g ⁻¹ 89%@500 th cycle	280 mAh g ⁻¹ @123 mAh g ⁻¹ 89%@500 th cycle	310 mAh g ⁻¹ @82 mAh g ⁻¹ 180 mAh g ⁻¹ @123 mAh g ⁻¹	[78b]
AM/CC/SSE = 20:10:70	Li ₆ PS ₅ Cl	60 °C	1.2–3.8 V 2.0/2.4 V (vs. Li ⁺ /Li)	178/ 225 mAh g ⁻¹ 79 %	180 mAh g ⁻¹ @18 mAh g ⁻¹ 94%@200 th cycle	180 mAh g ⁻¹ @18 mAh g ⁻¹ 94%@200 th cycle	160 mAh g ⁻¹ @42 mAh g ⁻¹ 162 mAh g ⁻¹ @42 mAh g ⁻¹	[78a]
PAQS	Na ₃ PS ₄	60 °C	1.0–3.1 V 1.3/1.7 V (vs. Li ⁺ /Li)	185/ 225 mAh g ⁻¹ 82 %	185 mAh g ⁻¹ @18 mAh g ⁻¹ 97%@200 th cycle	185 mAh g ⁻¹ @18 mAh g ⁻¹ 97%@200 th cycle	322 mAh g ⁻¹ @41 mAh g ⁻¹ 290 mAh g ⁻¹ @82 mAh g ⁻¹	[77]
PT	AM/SP/SSE = 25:25:50	Li ₇ P ₃ S ₁₁	60 °C	1.5–3.5 V 1.9/2.3 V (vs. Li ⁺ /Li)	310/ 317 mAh g ⁻¹ 98 %	310 mAh g ⁻¹ @32 mAh g ⁻¹ 91%@500 th cycle	304 mAh g ⁻¹ @32 mAh g ⁻¹ 91%@500 th cycle	[79]
PTTCA	+ S—N=N—S _n	25 °C	1.3–3.5 V 1.8/2.7 V (vs. Li ⁺ /Li)	410/ 450 mAh g ⁻¹ 91 %	410 mAh g ⁻¹ @50 mAh g ⁻¹ 83%@100 th cycle	410 mAh g ⁻¹ @50 mAh g ⁻¹ 83%@100 th cycle	415 mAh g ⁻¹ @50 mAh g ⁻¹ 335 mAh g ⁻¹ @100 mAh g ⁻¹	[32]
PMTH	AM/CNT ₅ /SP/SSE = 30:12.9:21.55	Li ₇ P ₃ S ₁₁	60 °C	1.3–3.5 V 2.0/2.7 V (vs. Li ⁺ /Li)	510/ 450 mAh g ⁻¹ 113 %	—	253 mAh g ⁻¹ @200 mAh g ⁻¹ 137 mAh g ⁻¹ @500 mAh g ⁻¹ 510 mAh g ⁻¹ @50 mAh g ⁻¹ 442 mAh g ⁻¹ @100 mAh g ⁻¹ 366 mAh g ⁻¹ @200 mAh g ⁻¹ 258 mAh g ⁻¹ @500 mAh g ⁻¹	[80]
PMTH	AM/SC65/SS _E = 33:17.50	Li ₆ PS ₅ Cl	25 °C	1.0–3.6 V 2.0/2.6 V (vs. Li ⁺ /Li)	595/ 597 mAh g ⁻¹ 100 %	592 mAh g ⁻¹ @60 mAh g ⁻¹ 91%@260 th cycle	610 mAh g ⁻¹ @70 mAh g ⁻¹ 500 mAh g ⁻¹ @230 mAh g ⁻¹ 460 mAh g ⁻¹ @390 mAh g ⁻¹ 341 mAh g ⁻¹ @710 mAh g ⁻¹	[80]

Active material	Cathode composition ^[a]	Solid-state electrolyte ^[b]	Testing temperature	Voltage window and average discharge/charge potential ^[c]	Reversible/theoretical capacity and utilization ^[d]	Cycling performance (reversible capacity @current rate and retention@cycle number) ^[e]	Rate performance (reversible capacity @current rate)	Ref.
PI	PI-G/SC65/SSE =50:10:40	Li ₈ PS ₃ Cl Na ₃ PS ₄	60 °C	1.4–3.6 V 2.1/2.5 V (vs. Li ⁺ /Li)	190/ 183 mAh g ⁻¹ 104 %	190 mAh g ⁻¹ @18 mAh g ⁻¹ 105 %@100 th cycle	195 mAh g ⁻¹ @9 mAh g ⁻¹ 130 mAh g ⁻¹ @36 mAh g ⁻¹ 100 mAh g ⁻¹ @78 mAh g ⁻¹ 90 mAh g ⁻¹ @104 mAh g ⁻¹	[84]

^[a] The electrode is composed of active material (AM), conductive carbon (CC), and solid-state electrolyte (SSE) or binder with specified weight ratio; the conductive carbons include Ketjen Black (KB), carbon nanotubes (CNTs), Super P (SP), porous carbon black (CB), acetylene black (AB), and Super C65 (SC65); the binders include poly(ethylene oxide)/poly(propylene oxide) copolymer (CPSEB) polyvinylidene fluoride (PVDF). ^[b] LICON-3 is a COF-based electrolyte containing –OLi and –SO₂Li functional groups. ^[c] The average potential is defined as the value of specific energy divided by specific capacity adopted from typical discharge/charge curves under relatively low current rate. ^[d] The data are adopted from the text or measured from the figures following the same standards as far as possible, which may be somewhat different from the claimed data but more objective for comparing the electrochemical performance in different references. Specifically, the reversible capacity is defined as the maximum discharge capacity after deducting the remarkable irreversible capacity (usually in the initial cycle). ^[e] The unit of current rate is converted into mAh g⁻¹ if the original unit “C” in the literature is clearly defined.

(e.g., P, Ge) of the SSE is too high, side reactions will also occur, leading to low capacity utilization, large irreversible capacity, and severe voltage polarization.

- 5) Cathode composition and structure. Due to the poor ionic and electronic conductivity of OCMs, they have to be highly dispersed and sufficiently contact with SSE and conductive carbon in the cathode to achieve high utilization. On one hand, it requires to increase the proportions of SSE (typically > 50 wt%) and conductive carbon (typically > 10 wt%) and decrease the proportion of OCM (typically < 40 wt%), which significantly reduce the practical energy density of the electrode and cell. On the other hand, the increased proportions of SSE and conductive carbon will inevitably enlarge their contact area and facilitate the electrochemical decomposition reactions of the SSE. To overcome these two drawbacks, it is required to enhance the effective contact of OCM with the limited SSE and conductive carbon as much as possible, and simultaneously reduce the unfavorable contact between the SSE and carbon. It is a huge challenge for the cathode fabrication, but may be realized by optimized mixing methods, *in-situ* composition of OCM and carbon, hierarchical structure designs, and percolation network designs for electron and ion.
- 6) All-solid-state or quasi-solid-state batteries. There is a lot of confusion about whether the reported SSBs in the literatures are actually all-solid-state, quasi-solid-state, or even gel batteries. The inaccurate categorization may lead to unfair comparison between different OCMs, SSEs, and battery systems, and even misunderstanding on the scientific issues. For SIE-based SSBs, if no solvent has been added in the fabrication process, or the added solvent (usually with low boiling point) has been completely removed (which can be verified by various characterization methods), there is no doubt that they belong to all-solid-state batteries. For SPE- and SCE-based SSBs, it is highly possible that they are not all-solid-state batteries as claimed because of many factors including residual solvent from the electrolyte and cathode preparation processes, liquid monomer from decomposed polymer (e.g., PPC), melted constituent (e.g., SCN) in the composite due to the anti-crystallization effect of other constituents. Even though it has been confirmed that there is no liquid at all at RT, the possibility cannot be excluded that the latter two factors produce some liquid at higher testing temperature, e.g. 60 °C. Moreover, at such a high temperature, it is still controversial whether the SPE (e.g., LiTFSI–PEO) can be regarded as solid because of the violent segmental motion of the polymer chains. The concept of all-solid-state batteries should be carefully used, because that a little liquid in the electrolyte and cathode can greatly improve the ionic conductivity and reduce the interface resistance. If necessary, it is acceptable to retain or add a certain amount of liquid in the SSB based on OCM, however, it should be claimed as a quasi-solid-state battery honestly.

Although there are so many problems for the application of OCMs in SSBs, the fundamental advantages and recent progress encourage further explorations in this field. Mean-

while, the achievements in the fields of OCMs, SSEs, SSBs based on inorganic cathode materials, and especially solid-state Li/Na–S batteries, can be learned to optimize the design and fabrication of SSBs based on OCMs. Advanced and ingenious *ex-situ* and *in-situ* characterization methods as well as high precise simulation and calculation methods, need to be established for in-depth understanding of the ionic and electronic conduction as well as interface structures and evolutions in the cathode during discharge-charge cycling. We believe that the rules and mechanisms of this system will be revealed step by step, and the electrochemical performance will be continually improved towards practical application.

Acknowledgements

The authors gratefully acknowledge financial support from the National Key Research and Development Program of China (2022YFB2402201), the National Natural Science Foundation of China (Nos. 21975189 and 22179102), and the Recruitment Program for Young Professionals.

Conflict of Interest

The authors declare no conflict of interest.

Data Availability Statement

Data sharing is not applicable to this article as no new data were created or analyzed in this study.

Keywords: lithium batteries • organic cathode materials • sodium batteries • solid-state batteries • solid-state electrolytes • sulfide electrolytes

- [1] M. Armand, J.-M. Tarascon, *Nature* **2008**, *451*, 652–657.
- [2] M. Winter, B. Barnett, K. Xu, *Chem. Rev.* **2018**, *118*, 11433–11456.
- [3] E. Fan, L. Li, Z. Wang, J. Lin, Y. Huang, Y. Yao, R. Chen, F. Wu, *Chem. Rev.* **2020**, *120*, 7020–7063.
- [4] C. Delmas, *Adv. Energy Mater.* **2018**, *8*, 1703137.
- [5] Y.-X. Yin, S. Xin, Y.-G. Guo, L.-J. Wan, *Angew. Chem. Int. Ed.* **2013**, *52*, 13186–13200.
- [6] W.-J. Kwak, Rosy, D. Sharon, C. Xia, H. Kim, L. R. Johnson, P. G. Bruce, L. F. Nazar, Y.-K. Sun, A. A. Frimer, M. Noked, S. A. Freunberger, D. Aurbach, *Chem. Rev.* **2020**, *120*, 6626–6683.
- [7] X. D. Chen, X. J. Yin, J. Aslam, W. W. Sun, Y. Wang, *Electrochim. Energy Rev.* **2022**, *5*, 12.
- [8] a) P. Poizot, J. Gaubicher, S. Renault, L. Dubois, Y. Liang, Y. Yao, *Chem. Rev.* **2020**, *120*, 6490–6557; b) Y. Liang, Y. Yao, *Joule* **2018**, *2*, 1690–1706.
- [9] Y. Lu, Q. Zhang, L. Li, Z. Q. Niu, J. Chen, *Chem* **2018**, *4*, 2786–2813.
- [10] Y. Lu, J. Chen, *Nat. Rev. Chem.* **2020**, *4*, 127–142.
- [11] R. Chen, Q. Li, X. Yu, L. Chen, H. Li, *Chem. Rev.* **2020**, *120*, 6820–6877.
- [12] J. Heiska, M. Nisula, M. Karppinen, *J. Mater. Chem. A* **2019**, *7*, 18735–18758.
- [13] a) L. Zhao, A. E. Lakraychi, Z. Chen, Y. Liang, Y. Yao, *ACS Energy Lett.* **2021**, *6*, 3287–3306; b) S. Wang, J. Lv, X. Wang, H. Cui, W. Huang, Y. Wang, *ChemElectroChem* **2021**, *9*, 9.
- [14] Z. Song, H. Zhou, *Energy Environ. Sci.* **2013**, *6*, 2280–2301.
- [15] P. J. Nigrey, D. MacInnes, D. P. Nairns, A. G. Macdiarmid, A. J. Heeger, *J. Electrochem. Soc.* **1981**, *128*, 1651–1654.
- [16] Z. Song, in *Redox Polymers for Energy and Nanomedicine*, Vol. 34 (Eds: N. Casado, D. Mecerreyres), The Royal Society of Chemistry, London, UK 2020, Ch. 6.
- [17] a) S. J. Visco, L. C. Dejonghe, *J. Electrochem. Soc.* **1988**, *135*, 2905–2909; b) D.-Y. Wang, W. Guo, Y. Fu, *Acc. Chem. Res.* **2019**, *52*, 2290–2300; c) Z. Shadike, S. Tan, Q.-C. Wang, R. Lin, E. Hu, D. Qu, X.-Q. Yang, *Mater. Horiz.* **2021**, *8*, 471–500.
- [18] a) C. Luo, X. Ji, S. Hou, N. Eidson, X. Fan, Y. Liang, T. Deng, J. Jiang, C. Wang, *Adv. Mater.* **2018**, *30*, e1706498; b) C. Luo, G.-L. Xu, X. Ji, S. Hou, L. Chen, F. Wang, J. Jiang, Z. Chen, Y. Ren, K. Amine, C. Wang, *Angew. Chem. Int. Ed.* **2018**, *57*, 2879–2883; c) C. Luo, O. Borodin, X. Ji, S. Hou, K. J. Gaskell, X. Fan, J. Chen, T. Deng, R. Wang, J. Jiang, C. Wang, *Proc. Natl Acad Sci U S A* **2018**, *115*, 2004–2009.
- [19] a) G. A. Snook, P. Kao, A. S. Best, *J. Power Sources* **2011**, *196*, 1–12; b) T. B. Schon, B. T. McAllister, P.-F. Li, D. S. Seferos, *Chem. Soc. Rev.* **2016**, *45*, 6345–6404.
- [20] K. Nakahara, S. Iwasa, M. Satoh, Y. Morioka, J. Iriyama, M. Suguro, E. Hasegawa, *Chem. Phys. Lett.* **2002**, *359*, 351–354.
- [21] a) K. Nakahara, K. Oyaizu, H. Nishide, *Chem. Lett.* **2011**, *40*, 222–227; b) S. Muench, A. Wild, C. Friebel, B. Haupler, T. Janoschka, U. S. Schubert, *Chem. Rev.* **2016**, *116*, 9438–9484.
- [22] a) H. Y. Chen, M. Armand, M. Courty, M. Jiang, C. P. Grey, F. Dolhem, J.-M. Tarascon, P. Poizot, *J. Am. Chem. Soc.* **2009**, *131*, 8984–8988; b) R.-h. Zeng, X.-p. Li, Y.-c. Qiu, W.-S. Li, J. Yi, D.-S. Lu, C.-I. Tan, M.-q. Xu, *Electrochim. Commun.* **2010**, *12*, 1253–1256; c) J. Lee, M. J. Park, *Adv. Energy Mater.* **2017**, *7*, 8; d) X. Wu, S. Jin, Z. Zhang, L. Jiang, L. Q. Mu, Y.-S. Hu, H. Li, X. Chen, M. Armand, L. Chen, X. Huang, *Sci. Adv.* **2015**, *1*, 9; e) S. Gottis, A.-L. Barres, F. Dolhem, P. Poizot, *ACS Appl. Mater. Interfaces* **2014**, *6*, 10870–10876; f) E. Deunf, P. Moreau, E. Quarez, D. Guyomard, F. Dolhem, P. Poizot, *J. Mater. Chem. A* **2016**, *4*, 6131–6139; g) A. Jouhara, N. Dupre, A.-C. Gaillot, D. Guyomard, F. Dolhem, P. Poizot, *Nat. Commun.* **2018**, *9*, 11; h) A. Shimizu, H. Kuramoto, Y. Tsujii, T. Nakami, Y. Inatomi, N. Hojo, H. Suzuki, J.-i. Yoshida, *J. Power Sources* **2014**, *260*, 211–217; i) S. Renault, S. Gottis, A.-L. Barres, M. Courty, O. Chauvet, F. Dolhem, P. Poizot, *Energy Environ. Sci.* **2013**, *6*, 2124–2133; j) A. E. Lakraychi, K. Fahsi, L. Aymard, P. Poizot, F. Dolhem, J.-P. Bonnet, *Electrochim. Commun.* **2017**, *76*, 47–50; k) A. E. Lakraychi, E. Deunf, K. Fahsi, P. Jimenez, J.-P. Bonnet, F. Djedaini-Pilard, M. Becuwe, P. Poizot, F. Dolhem, *J. Mater. Chem. A* **2018**, *6*, 19182–19189; l) W. Wan, H. Lee, X. Yu, C. Wang, K.-W. Nam, X.-Q. Yang, H. Zhou, *RSC Adv.* **2014**, *4*, 19878–19882.
- [23] a) H. Li, W. Duan, Q. Zhao, F. Cheng, J. Liang, J. Chen, *Inorg. Chem. Front.* **2014**, *1*, 193–199; b) D. J. Min, F. Miomandre, P. Audebert, J. E. Kwon, S. Y. Park, *ChemSusChem* **2019**, *12*, 503–510; c) J. E. Kwon, C.-S. Hyun, Y. J. Ryu, J. Lee, D. J. Min, M. J. Park, B.-K. An, S. Y. Park, *J. Mater. Chem. A* **2018**, *6*, 3134–3140.
- [24] a) Z. Gong, S. Zheng, J. Zhang, Y. Duan, Z. Luo, F. Cai, Z. Yuan, *ACS Appl. Mater. Interfaces* **2022**, *14*, 11474–11482; b) B. Wang, Y. Jin, Y. Si, W. Guo, Y. Fu, *Chem. Commun.* **2022**, *58*, 3657–3660; c) Z. Song, Y. Qian, M. Otani, H. Zhou, *Adv. Energy Mater.* **2016**, *6*, 7; d) H. Senoh, M. Yao, H. Sakaebe, K. Yasuda, Z. Siroma, *Electrochim. Acta* **2011**, *56*, 10145–10150.
- [25] a) T. Cai, Y. Han, Q. Lan, F. Wang, J. Chu, H. Zhan, Z. Song, *Energy Storage Mater.* **2020**, *31*, 318–327; b) H. Fei, Y. Liu, C. Wei, Y. Zhang, J. Feng, C. Chen, H. Yu, *Acta Phys. Chim. Sin.* **2020**, *36*, 6.
- [26] a) C. Guo, K. Zhang, Q. Zhao, L. Peia, J. Chen, *Chem. Commun.* **2015**, *51*, 10244–10247; b) W. Li, L. Chen, Y. Sun, C. Wang, Y. Wang, Y. Xia, *Solid State Ionics* **2017**, *300*, 114–119.
- [27] W. Huang, Z. Zhu, L. Wang, S. Wang, H. Li, Z. Tao, J. Shi, L. Guan, J. Chen, *Angew. Chem. Int. Ed.* **2013**, *52*, 9162–9166.
- [28] L. Chen, L. Cheng, J. Yu, J. Chu, H. G. Wang, F. Cui, G. Zhu, *Adv. Funct. Mater.* **2022**, *32*, 9.
- [29] M. Lécuyer, J. Gaubicher, A.-L. Barrès, F. Dolhem, M. Deschamps, D. Guyomard, P. Poizot, *Electrochim. Commun.* **2015**, *55*, 22–25.
- [30] W. Shi, J. Wang, X. Zhang, Q. Wang, W. Deng, *Int. J. Energy Res.* **2022**, *46*, 7686–7693.
- [31] M. Nisula, M. Karppinen, *J. Mater. Chem. A* **2018**, *6*, 7027–7033.
- [32] Z. Yang, F. Wang, Z. Hu, J. Chu, H. Zhan, X. Ai, Z. Song, *Adv. Energy Mater.* **2021**, *11*, 10.
- [33] a) R. Precht, R. Hausbrand, W. Jaegermann, *Phys. Chem. Chem. Phys.* **2015**, *17*, 6588–6596; b) B. Häupler, R. Burges, T. Janoschka, T. Jähnert, A. Wild, U. S. Schubert, *J. Mater. Chem. A* **2014**, *2*, 8999–9001.
- [34] X. Liu, Z. Ye, *Adv. Energy Mater.* **2020**, *11*, 13.

- [35] a) J. Wang, A. E. Lakraychi, X. Liu, L. Sieuw, C. Morari, P. Poizot, A. Vlad, *Nat. Mater.* **2021**, *20*, 665–673; b) J. Wang, X. Liu, H. Jia, P. Apostol, X. Guo, F. Lucaccioni, X. Zhang, Q. Zhu, C. Morari, J.-F. Gohy, A. Vlad, *ACS Energy Lett.* **2022**, *7*, 668–674.
- [36] a) Z. Chen, J. Wang, T. Cai, Z. Hu, J. Chu, F. Wang, X. Gan, Z. Song, *ACS Appl. Mater. Interfaces* **2022**, *14*, 27994–28003; b) R. Shi, L. Liu, Y. Lu, C. Wang, Y. Li, L. Li, Z. Yan, J. Chen, *Nat. Commun.* **2020**, *11*, 10.
- [37] T. Shi, G. Li, Y. Han, Y. Gao, F. Wang, Z. Hu, T. Cai, J. Chu, Z. Song, *Energy Storage Mater.* **2022**, *50*, 265–273.
- [38] Q. Zhao, S. Stalin, C.-Z. Zhao, L. A. Archer, *Nat. Rev. Mater.* **2020**, *5*, 229–252.
- [39] L.-Z. Fan, H. He, C.-W. Nan, *Nat. Rev. Mater.* **2021**, *6*, 1003–1019.
- [40] a) H. Kim, F. X. Wu, J. T. Lee, N. Nitta, H.-T. Lin, M. Oschatz, W. I. Cho, S. Kaskel, O. Borodin, G. Yushin, *Adv. Energy Mater.* **2015**, *5*, 8; b) J. Zheng, X. Fan, G. B. Ji, H. Wang, S. Hou, K. C. DeMella, S. R. Raghavan, J. Wang, K. Xu, C. Wang, *Nano Energy* **2018**, *50*, 431–440.
- [41] a) X. Feng, D. Ren, X. He, M. Ouyang, *Joule* **2020**, *4*, 743–770; b) Y. Guo, S. Wu, Y.-B. He, F. Kang, L. Chen, H. Li, Q.-H. Yang, *eScience* **2022**, 138–163.
- [42] Y. Benabed, M. Rioux, S. Rousselot, G. Hautier, M. Dollé, *Front. Energy Res.* **2021**, *9*, 13.
- [43] <https://www.szkejing.com/category-877.html>.
- [44] a) Y. Zhu, X. He, Y. Mo, *ACS Appl. Mater. Interfaces* **2015**, *7*, 23685–23693; b) F. Han, T. Gao, Y. Zhu, K. J. Gaskell, C. Wang, *Adv. Mater.* **2015**, *27*, 3473–3483.
- [45] Z. Sun, Y. Lai, N. Lv, Y. Hu, B. Q. Li, S. Jing, L. Jiang, M. Jia, J. Li, S. Chen, F. Liu, *Adv. Mater. Interfaces* **2021**, *8*, 8.
- [46] a) Y. Tian, T. Shi, W. Richards, J. Li, J. Kim, S.-H. Bo, G. Ceder, *Energy Environ. Sci.* **2017**, *10*, 1150–1166; b) Q. K. Zhang, F. Liang, Y. C. Yao, W. H. Ma, B. Yang, Y. N. Dai, *Prog. Chem.* **2019**, *31*, 210–222.
- [47] X. Li, J. Liang, X. Yang, K. R. Adair, C. Wang, F. Zhao, X. Sun, *Energy Environ. Sci.* **2020**, *13*, 1429–1461.
- [48] X. H. Yu, J. B. Bates, G. E. Jellison, F. X. Hart, *J. Electrochem. Soc.* **1997**, *144*, 524–532.
- [49] Z. Xue, D. He, X. Xie, *J. Mater. Chem. A* **2015**, *3*, 19218–19253.
- [50] a) K.-N. Jung, H.-S. Shin, M.-S. Park, J.-W. Lee, *ChemElectroChem* **2019**, *6*, 3842–3859; b) K. J. Kim, M. Balaish, M. Wadaguchi, L. Kong, J. L. M. Rupp, *Adv. Energy Mater.* **2021**, *11*, 63.
- [51] M. Faraday, *Philos. Trans. R. Soc. London* **1833**, 23–54.
- [52] J. Wolfenstine, J. L. Allen, J. Sakamoto, D. J. Siegel, H. Choe, *Ionics* **2018**, *24*, 1271–1276.
- [53] a) A. Sakuda, A. Hayashi, M. Tatsumisago, *Sci. Rep.* **2013**, *3*, 5; b) Z. Deng, Z. Wang, I.-H. Chu, J. Luo, S. P. Ong, *J. Electrochem. Soc.* **2016**, *163*, A67–A74.
- [54] J. Lu, J. Chen, T. He, J. Zhao, J. Liu, Y. Huo, *Prog. Chem.* **2021**, *33*, 1344–1361.
- [55] J. D. LaCoste, A. Zakutayev, L. Fei, *J. Phys. Chem. C* **2021**, *125*, 3651–3667.
- [56] J. Mindemark, M. J. Lacey, T. Bowden, D. Brandell, *Prog. Polym. Sci.* **2018**, *81*, 114–143.
- [57] Y. Zheng, Y. Yao, J. Ou, M. Li, D. Luo, H. Dou, Z. Li, K. Amine, A. Yu, Z. Chen, *Chem. Soc. Rev.* **2020**, *49*, 8790–8839.
- [58] K. J. Kim, J. L. M. Rupp, *Energy Environ. Sci.* **2020**, *13*, 4930–4945.
- [59] a) W. Jiang, L. Yan, X. Zeng, X. Meng, R. Huang, X. Zhu, M. Ling, C. Liang, *ACS Appl. Mater. Interfaces* **2020**, *12*, 54876–54883; b) S. J. Guo, Y. T. Li, B. Li, N. S. Grundish, A.-M. Cao, Y.-G. Sun, Y. S. Xu, Y. L. M. Ji, Y. Qiao, Q. H. Zhang, F. Q. Meng, Z.-H. Zhao, D. Wang, X. Zhang, L. Gu, X. Q. Yu, L.-J. Wan, *J. Am. Chem. Soc.* **2022**, *144*, 2179–2188.
- [60] a) S.-S. Chi, Y. Liu, N. Zhao, X. Guo, C.-W. Nan, L.-Z. Fan, *Energy Storage Mater.* **2019**, *17*, 309–316; b) Z. Lu, Z. Yang, C. Li, K. Wang, J. Han, P. Tong, G. Li, B. S. Vishnugoppi, P. P. Mukherjee, C. Yang, W. Li, *Adv. Energy Mater.* **2021**, *11*, 10.
- [61] a) C. Wang, X. Sun, L. Yang, D. Song, Y. Wu, T. Ohsaka, F. Matsumoto, J. Wu, *Adv. Mater. Interfaces* **2021**, *8*, 10; b) X. Pan, H. Sun, Z. Wang, H. Huang, Q. Chang, J. Li, J. Gao, S. Wang, H. Xu, Y. Li, W. Zhou, *Adv. Energy Mater.* **2020**, *10*, 11.
- [62] D. Cao, Y. Zhang, A. M. Nolan, X. Sun, C. Liu, J. Sheng, Y. Mo, Y. Wang, H. Zhu, *Nano Lett.* **2020**, *20*, 1483–1490.
- [63] Y. Cui, Z. Zhang, Y. Huang, J. Lin, X. Yao, X. Xu, *Energy Storage Science and Technology* **2021**, *10*, 836.
- [64] M. L. Liu, S. J. Visco, L. C. Dejonghe, *J. Electrochem. Soc.* **1991**, *138*, 1891–1895.
- [65] M. Lécuyer, M. Deschamps, D. Guyomard, J. Gaubicher, P. Poizot, *Molecules* **2021**, *26*, 14.
- [66] a) C. Wang, H. Zhang, J. Li, J. Chai, S. Dong, G. Cui, *J. Power Sources* **2018**, *397*, 157–161; b) J. Li, S. Dong, C. Wang, Z. Hu, Z. Zhang, H. Zhang, G. Cui, *J. Mater. Chem. A* **2018**, *6*, 11846–11852.
- [67] B. Kim, H. Kang, K. Kim, R.-Y. Wang, M. J. Park, *ChemSusChem* **2020**, *13*, 2271–2279.
- [68] X. Li, Q. Hou, W. Huang, H.-S. Xu, X. Wang, W. Yu, R. Li, K. Zhang, L. Wang, Z. Chen, K. Xie, K. P. Loh, *ACS Energy Lett.* **2020**, *5*, 3498–3506.
- [69] K. Hatakeyama-Sato, T. Tezuka, R. Ichinoi, S. Matsumono, K. Sadakuni, K. Oyaizu, *ChemSusChem* **2020**, *13*, 2443–2448.
- [70] P. Leung, J. Bu, P. Q. Velasco, M. R. Roberts, N. Grobert, P. S. Grant, *Adv. Energy Mater.* **2019**, *9*, 12.
- [71] Z. Zhu, M. Hong, D. Guo, J. Shi, Z. Tao, J. Chen, *J. Am. Chem. Soc.* **2014**, *136*, 16461–16464.
- [72] X. Chi, F. Hao, J. Zhang, X. Wu, Y. Zhang, S. Gheytani, Z. Wen, Y. Yao, *Nano Energy* **2019**, *62*, 718–724.
- [73] N. Wu, P.-H. Chien, Y. Qian, Y. Li, H. Xu, N. S. Grundish, B. Xu, H. Jin, Y.-Y. Hu, G. Yu, J. B. Goodenough, *Angew. Chem. Int. Ed.* **2020**, *59*, 4131–4137.
- [74] F. Hao, Y. Liang, Y. Zhang, Z. Chen, J. Zhang, Q. Ai, H. Guo, Z. Fan, J. Lou, Y. Yao, *ACS Energy Lett.* **2021**, *6*, 201–207.
- [75] C. Luo, X. Ji, J. Chen, K. J. Gaskell, C. He, Y. Liang, J. Jiang, C. Wang, *Angew. Chem. Int. Ed.* **2018**, *57*, 8567–8571.
- [76] X. Yang, Y. Hu, N. Dunlap, X. Wang, S. Huang, Z. Su, S. Sharma, Y. Jin, F. Huang, X. Wang, S.-h. Lee, W. Zhang, *Angew. Chem. Int. Ed.* **2020**, *59*, 20385–20389.
- [77] W. Ji, X. Zhang, L. Xin, A. Luedtke, D. Zheng, H. Huang, T. Lambert, D. Qu, *Energy Storage Mater.* **2022**, *45*, 680–686.
- [78] a) F. Hao, Y. Liang, Y. Zhang, Z. Chen, J. Zhang, Q. Ai, H. Guo, Z. Fan, J. Lou, Y. Yao, *ACS Energy Lett.* **2020**, *6*, 201–207; b) F. Hao, X. Chi, Y. Liang, Y. Zhang, R. Xu, H. Guo, T. Terlier, H. Dong, K. Zhao, J. Lou, Y. Yao, *Joule* **2019**, *3*, 1349–1359; c) J. Zhang, Z. Chen, Q. Ai, T. Terlier, F. Hao, Y. Liang, H. Guo, J. Lou, Y. Yao, *Joule* **2021**, *5*, 1845–1859.
- [79] X. Zhou, Y. Zhang, M. Shen, Z. Fang, T. Kong, W. Feng, Y. Xie, F. Wang, B. Hu, Y. Wang, *Adv. Energy Mater.* **2022**, *12*, 11.
- [80] W. Ji, X. Zhang, D. Zheng, H. Huang, T. H. Lambert, D. Qu, *Adv. Funct. Mater.* **2022**, *32*, 11.
- [81] S. Zhang, Z. Li, L. Cai, Y. Li, V. G. Pol, *Chem. Eng. J.* **2021**, *416*.
- [82] W. Wei, L. Li, L. Zhang, J. Hong, G. He, *Electrochem. Commun.* **2018**, *90*, 21–25.
- [83] X. Chi, Y. Liang, F. Hao, Y. Zhang, J. Whiteley, H. Dong, P. Hu, S. Lee, Y. Yao, *Angew. Chem. Int. Ed.* **2018**, *57*, 2630–2634.
- [84] W. Ji, X. Zhang, H. Qu, L. Xin, A. T. Luedtke, H. Huang, T. H. Lambert, D. Qu, *Nano Energy* **2022**, *96*, 8.

Manuscript received: January 1, 2023

Revised manuscript received: January 30, 2023

Accepted manuscript online: January 31, 2023

Version of record online: March 10, 2023